Disruption of the La(III)[15-Metallacrown-5] Cavity through Bithiophene Dicarboxylate Inclusion

Joseph Jankolovits, Choong-Sun Lim, Jeff W. Kampf, and Vincent L. Pecoraro

Department of Chemistry, Willard H. Dow Laboratories, The University of Michigan, Ann Arbor, MI 48109-1055, USA

Reprint requests to Prof. Vincent L. Pecoraro. Fax: (+1) 734-647-4865. E-mail: vlpec@umich.edu

Z. Naturforsch. **2010**, *65b,* 263 – 272; received December 17, 2009

This article is dedicated to Professor Rolf W. Saalfrank in honor of his many productive years in the field of metallosupramolecular chemistry. His work has provided a major contribution to our understanding of this beautiful field of chemistry.

The inclusion of bithiophene dicarboxylate (btDC) in La(III)[15-MC$_{Cu,N,L\text{-phenylalaninehydroximate}}$-5] hosts (LaMC) unexpectedly results in a clathratocomplex with a completely disrupted hydrophobic cavity. Structures best formulated as $\{(LaMC)_2(\mu_2\text{-O})\}$ are formed that dimerize across the hydrophilic parts. This dimer appears stabilized by 5 phenyl-DMF-phenyl interactions and 10 DMF-amine hydrogen bonds. Electrospray ionization mass spectrometry reveals the presence of 2 : 2 LaMC-btDC complexes in solution. In the solid state, both *cis*- and *trans*-bithiophene dicarboxylate guests bridge the > 17 Å distance between LaMC hydrophobic faces. The resulting solid has over 50 % void space, suggesting guest-length and solvent considerations can predictably lead to the formation of open LaMC coordination frameworks or close-packed molecular compartments.

Key words: Metallacrown, Molecular Recognition, Host-Guest Chemistry, Bithiophene, Metallamacrocycle

Introduction

Supramolecular cation hosts have classically been based on organic macrocycles such as crown ethers [1, 2], cryptands [3], and carcerands [4]. More recently, chemists such as Prof. Rolf Saalfrank (Fig. 1) have applied the principles of the macrocyclic effect to create novel cation hosts by incorporating direct metal coordination into macrocycles. Metallacoronates [5 – 8], metallacryptates [9 – 12], and metallacrowns [13 – 23] are particular examples of macrocycles that contain metals in the ring structure and demonstrate cation binding through electron-rich ring donor atoms. Such metallamacrocycles have certain advantages over their organic counterparts. The donor atoms often possess a negative charge, which imparts stronger binding and the ability to recognize transition metals in the central cavity. Additionally, the ring metals can impart interesting spectroscopic and magnetic properties [24 – 30]. Lastly, the Lewis acidic ring metals provide additional binding sites for anions that permit coordination modes that are not possible in organic macrocycles [31 – 39], and can lead to exciting molecular architectures through, as Prof. Saalfrank has eloquently stated, "the synergistic effects of serendipity and rational design" [40].

Fig. 1. Rolf Saalfrank (left) and Al Crumbliss during a break in scientific sessions at the Sonderforschungsbereich on "Metal Mediated Reactions Modelled after Nature", at Friedrich-Schiller-University and the Max Planck Institute of Chemical Ecology, in Jena, Germany, September, 2005.

Much of the interest in metallamacrocycles lies in the solid-state materials templated by the metal-rich

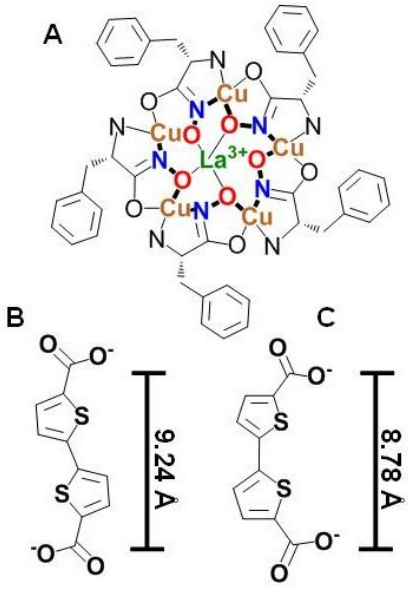

Fig. 2. A: A ChemDraw representation of La(III)[15-MC-5]. B: *trans*-btDC. C: *cis*-btDC. Displayed lengths are measured from carboxylate-carbon to carboxylate-carbon in the crystal structure.

host and guest molecules. In particular, metallacrown host-guest complexes have been used to create functional crystalline solids exhibiting micro- and mesoporosity [41, 42], second-harmonic generation [43], and selective guest absorption at the solid-liquid interface [44]. 15-Metallacrown-5 complexes [45 – 47] derived from α-amino hydroxamic acid ligands, copper ring metal atoms, and an encapsulated lanthanide central atom (Fig. 2A) are metallamacrocycles that exemplify the advantages of construction through metal coordination. They bind the central lanthanide strongly and are quite stable [48 – 50]. They also have interesting magnetic properties, with a Dy(III) analog possessing single-molecule magnetism [51]. Additionally, they are exciting anion recognition agents, exhibiting selective guest binding in solution and in the solid state [52 – 55].

The solid-state structures of Ln^{3+}[15-MC-5] complexes synthesized with L-phenylalanine hydroxamic acid ligands (L-pheHA, *Ln*MCs, Fig. 2A) possess molecular compartments as the defining feature. These compartments result from the dimerization of *Ln*MC cavities *via* π-π interactions between the pheHA side chains. In order to maximize these interactions, the compartments typically possess cylindrical geometry and a height of around 11.5 Å (measured by the *Ln*–*Ln* distance). With appropriate templating anions, however, exotic *Ln*MC assemblies have been serendipitously realized. For example, GdMCs crystallized with nitrate in methanolic solutions give rise to resolved helices [56, 57], while LaMCs with pimelate or suberate guest anions template a mesostructured array of octameric LaMC compartments [44]. Additionally, resolved metallahelicates were synthesized with norvaline hydroxamic acid in the absence of a lanthanide [58].

Generally, guest binding by *Ln*MC compartments follows "rational design" principles, selectively encapsulating unsaturated guests based on size and guest-ligand interactions [59, 60]. We demonstrated that terephthalate and muconate were sequestered by the compartments, as their length (5.78 and 6.27 Å, respectively, measured by the carboxylate-carbon to carboxylate-carbon distance) was complementary with the optimal 11.5 Å compartment size. However, the compartment was disrupted by naphthalene dicarboxylate (naphDC) as the long guest (8.00 Å) disrupted the π-π interactions necessary for compartment integrity. As a result, the guest was bound in individual *Ln*MC cavities, which slid horizontally by 11 Å relative to each other. Phenyl rings on adjacent *Ln*MC cavities maintained π-π interactions so that an 11.5 Å vertical separation was observed between *Ln*MCs.

*Ln*MCs are a promising platform for designing functional crystalline solids, as the compartment can be used to predictably control the environment and orientation of guest molecules with interesting properties, such as NLO chromophores [43]. Typically, such functional guests are as large, or larger, than naphDC. Thus, we are interested in further investigating the inclusion of large guests to establish the rational design principles that govern inclusion phenomena in disrupted compartments. With this aim, we investigated the inclusion of bithiophene dicarboxylate (btDC, Fig. 2B, C). With a length of 9.24 Å, btDC is longer than naphDC and, therefore, was expected to prevent *Ln*MC dimerization. Herein we characterize the LaMC-btDC complex (**1**) by X-ray crystallography and electrospray ionization mass spectrometry (ESI-MS) and describe how its features shape the rational design principles of *Ln*MC-guest complexes.

Results

The reaction of bithiophene dicarboxylate disodium salt with La(III)$(NO_3)_{2.5}$[15-$MC_{Cu(II),N,L-pheHA}$-5]-

Table 1. Crystal structure data for **1**.

Formula	$La_2Cu_{10}C_{161}H_{254}N_{33.5}O_{68.75}S_6$
M_r	4864.56
Crystal size, mm^3	$0.35 \times 0.18 \times 0.08$
Crystal system	triclinic
Space group	$P\bar{1}$ (no. 1)
a, Å	18.9742(12)
b, Å	19.8779(13)
c, Å	20.2834(13)
α, deg	93.587(1)
β, deg	111.320(1)
γ, deg	114.263(1)
V, $Å^3$	6291.6(7)
Z	1
D_{calcd}, $g\,cm^{-3}$	1.28
$\mu(MoK_\alpha)$, cm^{-1}	12.8
$F(000)$, e	2504
hkl range	±25, ±26, ±27
$((\sin\theta)/\lambda)_{max}$, $Å^{-1}$	0.6677
Refl. measured / unique / R_{int}	203556 / 62188 / 0.0329
Param. refined	3169
$R(F)/wR(F^2)$ (all refl.)	0.0643 / 0.1535
x(Flack)	−0.022(7)
GoF (F^2)	1.080
$\Delta\rho_{fin}$ (max / min), $e\,Å^{-3}$	1.40 / −0.90

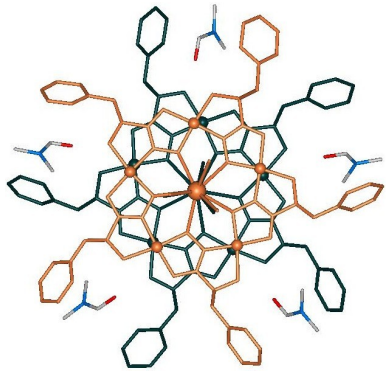

Fig. 3. The μ_2-oxide LaMC dimer shown from the top view. Bound solvent and btDC molecules were removed for clarity. Color scheme (color online): gold – top LaMC, dark grey – bottom LaMC, red – DMF oxygen, blue – DMF nitrogen, light grey – DMF carbon. Bound guests were removed for clarity.

$(NO_3)_{0.5}$ yielded crystals of **1** upon slow evaporation of an aqueous dimethylformamide (DMF) solution. X-Ray crystal structure analysis has revealed that 3 btDC anions are included per two LaMCs. Each La(III) is nine-coordinate with three water molecules bound on the hydrophilic face. The hydrophilic faces of two LaMCs stack on top of each other (Fig. 3), with an oxygen atom bridging the two La(III) central metals. The nearly linear La–O–La bond angle of 169.6° suggests that this bridging oxygen atom is

Table 2. Selected bond lengths (Å), angles (deg), and dihedral angles (deg) for **1** with estimated standard deviations in parentheses. The corresponding atoms are labeled in Fig. 4 or in the Supporting Information (Figs. S1 and S2). Atoms labeled with the subscript a are located on a disordered *trans*-btDC guest that is not shown.

La_1–O_1	2.617(2)	La_1–O_2	2.500(2)
La_1–O_3	2.525(2)	La_1–O_4	2.574(2)
La_1–$O_{MC-average}$	2.561(2)	La_2–O_1	2.624(2)
La_2–O_5	2.506(2)	La_2–O_6	2.551(2)
La_2–O_7	2.571(2)	La_2–$O_{MC-average}$	2.564(2)
Cu_1–O_8	2.416(1)	Cu_6–O_{11}	2.358(2)
Cu_3–O_{14}	2.419(2)	Cu_8–O_{15}	2.455(2)
O_2–O_{12}	2.590(7)	O_2–O_{13}	3.221(5)
O_2–O_{13a}	2.775(5)	O_3–O_{13}	2.846(6)
O_3–O_{13a}	2.797(6)	O_4–O_{13}	2.636(7)
O_4–O_{12a}	2.609(6)	O_5–O_{10}	2.713(4)
O_6–O_{10}	2.715(4)	O_7–O_9	2.685(4)
La_1–O_1–La_2	169.61(12)		
S_1–C_1–C_2–S_2	179.70(17)	S_3–C_3–C_4–S_4	178.8(4)
S_{3a}–C_{3a}–C_{4a}–S_{4a}	143.8(4)	S_5–C_5–C_6–S_6	21.4(4)

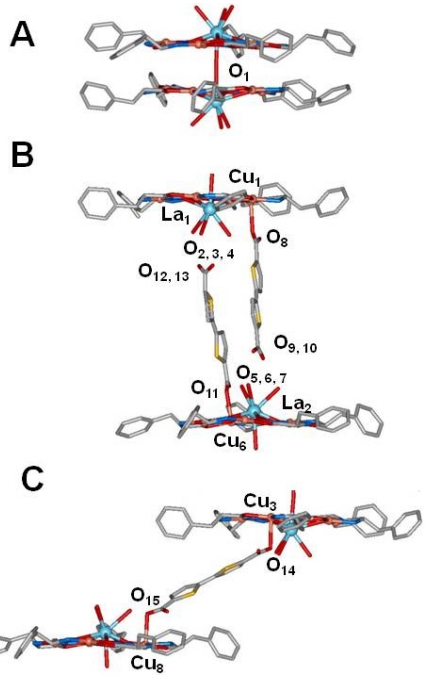

Fig. 4. Images of the various guest-bridged dimers observed in **1**. A: μ_2-oxide hydrophilic dimer. B: *trans*-btDC dimer. C: *cis*-$HbtDC^-$ dimer. Color scheme (color online): grey – carbon, yellow – sulfur, red – oxygen, blue – nitrogen, orange – copper, light blue – lanthanum. Atom labels are included that are utilized in Table 2.

an oxide [61]. The largest La–oxygen–La bond angle we have observed with a hydroxide or water bridge is 151° [62], though angles closer to 110° are more

often reported [63 – 65]. However, the La–O bond lengths (~ 2.62 Å) are more consistent with La(III)-OH_2 distances. Unit cell charge balance does not uniquely address this issue as the btDC guests have the capacity to carry protons. The long La–O bond probably result from sterics involving the La(III) ions and the two metallacrowns. The La(III)–La(III) distance in this dimer is ~ 5.22 Å, with the La(III) atoms being displaced into the hydrophobic face by ~ 0.78 Å from the metallacrown-oxygen mean plane (Fig. 4A). La(III) is too large to fit in the metallacrown plane, and the three coordinated water molecules pull it to the hydrophobic face. The closest possible approach between two parallel LaMCs is limited to a van der Waals separation, which is consistent with the observed 3.7 Å separation between LaMC faces. Since the distance between the two La(III) atoms could not get any shorter, the bridging oxide bond lengths are exceptionally long, even though the oxygen carries a -2 charge. Additionally, no electron density corresponding to a hydrogen atom bound to the bridging oxygen could be found. Given the disparity between the observed bond angle and the hydroxide or water bond angles from the literature, we feel the best formulation of this oxygen atom is as a μ_2-oxide although these other formulations are possible.

The bridging oxide is isolated from solution by the two disk-like MCs, which have an 11.7 Å radius from the central metal to the tips of the phenyl rings. Interstitial DMF molecules also bridge the two LaMCs through hydrogen bonds to amines on the periphery of both LaMCs (Fig. 3). Each interstitial DMF is hydrogen bonded (Fig. 5) through its oxygen atom to two amines on different LaMCs with O–NH_2 distances of ~ 2.9 Å. Unusually, the ligand side-chains are completely splayed out, resulting in the complete disruption of the hydrophobic cavity. With separations of $\sim 4.2 - 7$ Å, the splayed-out phenyl rings are not involved in π-π interactions across the hydrophilic faces. This is because the methylene groups are oriented towards the hydrophobic face. Instead, the rings are bridged by interstitial DMF molecules. Each hydrogen-bonded DMF molecule is sandwiched between two phenyl rings *via* an electrostatic interaction between the electron deficient aldehyde carbon on the hydrogen-bonded DMF molecule and the electron rich phenyl ring (Fig. 5). The distances from the aldehyde carbon to the center of the ring range from ~ 3.45 to 3.9 Å, which is similar to distances observed with phenyl T-stacking interactions [66, 67]. Thus the interstitial DMF molecules stabilize the hydrophilic dimer through interactions with LaMC amines and phenyl rings.

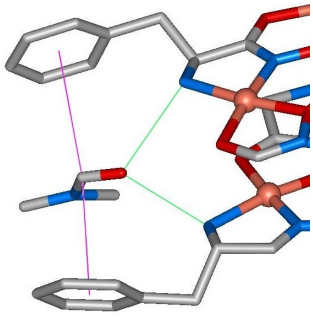

Fig. 5. Highlight of the interstitial DMF interactions with the μ_2-oxide LaMC dimer. The DMF oxygen forms hydrogen bonds with amines on both LaMCs (green), and interacts with the electron-rich phenyl rings *via* a stacking interaction with its electron-deficient aldehyde carbon (purple). Color scheme (color online): grey – carbon, red – oxygen, blue – nitrogen, orange – copper.

Charge balance is achieved in **1** with the bridging oxide and the btDC guests. The two LaMCs give a $+6$ charge. The oxide has a -2 charge. The *cis*-btDC guest carries a single proton, as does the planar *trans*-btDC guest on its unbound carboxylate. The two $HbtDC^-$ and $btDC^{2-}$ guests give overall charge neutrality.

On the hydrophobic face of each LaMC, a btDC guest is coordinated perpendicularly to a Cu(II) ring metal through a carboxylate oxygen atom (Fig. 4B). The unbound btDC carboxylate has hydrogen-bonding interactions with water coordinated to the central metal of an adjacent LaMC. The carboxylate-carbon to carboxylate-carbon distance on this btDC is 9.24 Å. This leaves a 15.99 Å La(III)–La(III) separation across the hydrophobic faces of adjacent MC's bridged by these btDC guests. The thiophene groups are *trans* to each other, which is the more stable orientation. In solution, the relative populations of *trans*- and *cis*-bithiophene is 56 % and 44 %, respectively [68 – 70]. The monoprotonated anion *trans*-$HbtDC^-$ is planar with a torsion angle of 179.7°, while the completely deprotonated *trans*-$btDC^{2-}$ guest is disordered between planar and twisted conformations, with torsion angles of 178.8° and 143.8°, respectively.

The third btDC is also coordinated to a Cu(II) ring metal, though this guest lies at an acute angle with the MC face. The $HbtDC^-$ guest bridges a Cu(II) on a neighboring LaMC, coordinating to both hosts with a single carboxylate oxygen atom (Fig. 4C). Notably, this $HbtDC^-$ is in the less stable *cis* conformation.

The steric interactions between the hydrogen atoms on the thiophene carbon atoms results in a 21.4° twisting of the thiophene rings, which is within the range typically observed for *cis*-bithiophenes [71 – 77]. The Cu–Cu distance bridged by this *cis*-btDC^{2-} is 14.10 Å, with a 10.94 Å distance between coordinating oxygen atoms. The La(III)–La(III) distance of the bridged LaMCs is 16.80 Å, which is the largest *Ln–Ln* distance between guest-bridged *Ln*MCs that has been reported to date. However, a cylindrical molecular compartment does not form, evidenced by the significant horizontal displacement of the LaMCs relative to each other. Interestingly, the dipole moments in all *cis*-HbtDC^{-} anions are oriented in the same direction in **1**, which gives the solid a net dipole. This is the second example of a *Ln*MC host-guest complex that forms a dipolar crystalline solid [43].

The coordination of the *cis*- and *trans*-btDC guests to nearby oxide-bridged LaMCs propagates through the structure (Fig. 6). The only direct coordination between LaMCs is the bridging *cis*-btDC^{2-} and oxide through the *b* axis. Packing forces, *trans*-btDC coordination and hydrogen bonding maintain the structure in the other directions. Notably, **1** contains a 9.73 × 15.86 Å^2 solvent channel down the *c* axis (Fig. 7). The channel is templated by *cis*-HbtDC^{-} and *trans*-btDC on the short axis and hydrophobic interactions between LaMC ligands on the long axis. **1** has a potential void space of 51.6 % accessible to guest molecules [78].

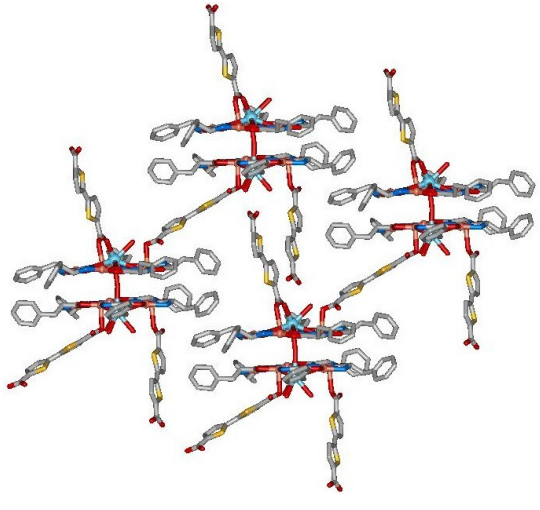

Fig. 6. Packing diagram of **1** displaying the bridging *cis*-HbtDC^{-}, *trans*-btDC and oxide linkages between LaMCs. Solvent molecules were removed for clarity. Color scheme (color online): grey – carbon, yellow – sulfur, red – oxygen, blue – nitrogen, orange – copper, light blue – lanthanum.

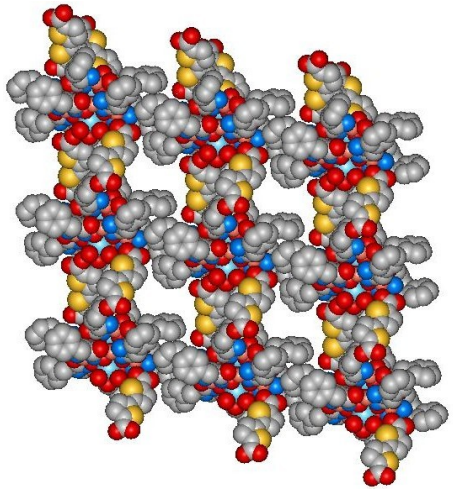

Fig. 7. CPK representation of **1** displaying the 9.73 × 15.86 Å^2 channels formed through hydrophobic L-pheHA interactions (horizontal) and coordination of the bridging btDC (vertical) to LaMC (intersection). Color scheme (color online): grey – carbon, yellow – sulfur, red – oxygen, blue – nitrogen, orange – copper, light blue – lanthanum.

1 was studied by electrospray ionization mass spectrometry (ESI-MS) in order to find out what species are present in solution (Fig. S3, S4; Supporting Information available online. See note at the end of the article). A solution containing **1** dissolved in a 4 : 1 DMF water mixture displayed peaks centered at *m/z* = 800.5 and 837, corresponding to the LaMC-btDC^{2+} and LaMC-btDC-DMF^{2+} ions. Additionally, a peak at *m/z* = 1600 was observed with half integer peaks, revealing a $LaMC_2$-$btDC_2{}^{2+}$ ion. The LaMC-btDC^{1+} ion would appear at the same mass and likely is also present, though the half integer peaks unambiguously demonstrate the presence of a LaMC dimer with two btDC guests. No peaks for a μ_2-oxide-LaMC complex were observed.

Discussion

We investigated the inclusion of btDC to learn more about the recognition of long guests in disrupted *Ln*MC compartments. X-Ray crystallography revealed that, as expected, a compartment structure was not observed with btDC. Surprisingly, the btDC guest not only disrupted the compartment, but the hydrophobic cavity as well (Fig. 3). **1** is the first example of an *Ln*MC containing the pheHA ligand that does not form a hydrophobic cavity. Instead, an unprecedented μ_2-oxide hydrophilic dimer is observed, with 5 interstitial DMF

molecules stabilizing the structure. It should be noted that Tegoni [79] has recently reported that the pK_a of water bound to *Ln*[15-MC-5] complexes is $\sim$ 4.5. This suggests that under neutral aqueous solution conditions this oxygen is found as a hydroxide and in basic, non-protic DMF this form would be stabilized. It is reasonable to expect that coordination of a second highly Lewis-acidic *Ln*(III) ion would acidify the remaining proton leading to the observed μ_2-O ligand that spans the two metallacrowns. Generally, *Ln*MC clathratocomplexes are crystallized from water/alcohol solutions which have high proton concentrations compared to DMF, which could explain why this structure has not been characterized in these protic solvents previously. The bridging oxide is likely an essential feature of this dimer (Fig. 4A). For the DMF molecules to act as a bridge in these conditions, the hydrophilic faces must assemble as close to one another as possible, which requires they are bridged by a single oxygen atom. If that oxygen atom came from a carboxylate, DMF, water, or hydroxide, the MC faces would either be bent relative to one another or be further apart in order to accommodate the molecule between the two MC faces. This would disrupt some or all of the bridging DMF interactions and likely prevent the hydrophilic faces from dimerizing.

The disruption of the hydrophobic cavity creates some interesting structural features. First, it allows numerous hydrophilic residues to bind at the hydrophobic face, which would normally be limited due to unfavorable interactions with the phenyl rings. Water molecules, nitrates, or carboxylates are always observed bound to metals in the hydrophobic cavity, and a carboxylate engaged in hydrogen bonds to coordinated water has been observed with a fumarate guest. However, the number of hydrophilic residues in **1** is unprecedented. There are three water molecules bound to La, two carboxylates bound to ring metals, a carboxylate hydrogen-bonded to the La-coordinated waters, water and DMF coordinated near the face, and the hydrophilic sulfur on btDC. Clearly the elimination of the hydrophobic cavity has eliminated the amphiphilic selectivity normally afforded by *Ln*MCs.

An additional feature of the cavity disruption is that the phenyl side chains do not enforce a particular guest orientation. Normally, guests extend roughly perpendicular to the MC plane, or are mostly contained within the cavity. This is due to the steric confines of the cavity and intermolecular interactions with the phenyl rings. However, the *cis*-HbtDC$^-$ guest extends sideways at a very acute angle relative to the LaMC plane in this structure (Fig. 4C). The promiscuity of the disrupted LaMC hydrophobic cavity could lead to a variety of interesting solid-state architectures.

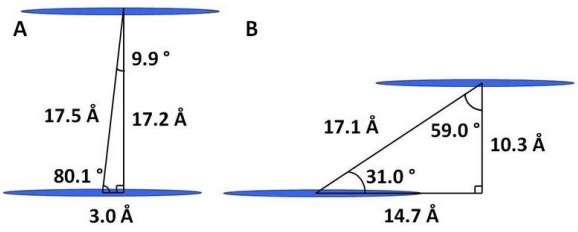

Fig. 8. Diagrams displaying the geometry of the *trans*- (A) and *cis*-btDC (B) clathratocomplexes. The hypotenuse is the distance between the centers of the LaMC faces, which is determined by the center of the mean-plane created by the ring oxygen atoms.

The lack of a cavity also generates major changes to the size of the resulting clathratocomplexes formed between LaMC and btDC on the hydrophilic face. Typically, interactions between hydrophobic cavities are a dominant factor in dictating the relative orientations of the hydrophobic faces of the *Ln*MC, typically resulting in $\sim$ 11.5 Å separations. However, the cavity disruption leads guest length to dictate the packing of the hydrophobic faces, which results in very large La(III)–La(III) distances. The two *trans*-btDC guests bridge the hydrophobic faces through copper coordination and hydrogen bonding. The resulting 15.99 Å La–La distance is greater than any previously reported values (Fig. 4B). Notably, the La(III)–La(III) distance between LaMCs bridged by *cis*-HbtDC$^-$ is even longer at 16.8 Å due to guest coordination to ring metals (Fig. 4C). When one considers that La(III) sits $\sim$ 0.78 Å above the hydrophobic face in this structure, the LaMC separations become even longer. Fig. 8 shows structural diagrams for the *trans*- and *cis*-btDC bridged clathratocomplexes with distances measured from the center of the LaMC faces. Both the *trans*- and *cis*-btDC dimers exhibit similar LaMC separations of 17.5 and 17.1 Å, respectively; however, the 14.7 Å horizontal displacement of the LaMCs with the *cis*-HbtDC$^-$ guest results in a significantly different shape. The range of sizes observed in *Ln*MC clathratocomplexes demonstrates the host's remarkable versatility.

Lastly, cavity disruption also contributes to the formation of a 9.73 $\times$ 15.86 Å solvent channel (Fig. 7), which is significant considering the interest in microporous systems such as metal-organic frameworks and

tectons [80, 81]. Generally, the strong π-π interactions between adjacent LaMC hydrophobic cavities leads to a very tightly packed structure, though there are exceptions to this that depend on how the guest is oriented on the hydrophilic face. Interestingly, the disruption of the hydrophobic cavity in **1** leads to the formation of a structure with 51.6 % void space accessible to guest molecules. This is greater than the 42.8 % void space reported for a mesostructured LaMC assembly generated through the packing of hydrophobic cavities and compartments [44]. Interestingly, nano-scale channels have now been templated in *Ln*MCs by guests binding exclusively to the hydrophilic [44] or hydrophobic face. The structure is suggestive of a general design principle for designing solids from *Ln*MC building blocks. Inclusion complexes with shorter guests grown from water/alcohol solutions have generally led to closely packed assemblies of molecular compartments. However, the utilization of an excessively long guest in DMF has led to the formation of a solid with over 50 % void space. Thus one could promote the formation of an open crystalline framework or close-packed molecular compartments through considerations of guest length and solvent.

Given their similar size, it is worth assessing why cavity disruption was observed with btDC, but not with naphDC. Guest length, hydrophilicity, and the crystallization solvent are important factors. *trans*-btDC is 1.24 Å longer than naphDC, which results in significant differences in how they are packed in the structure. With naphDC bound on the hydrophobic face, the cavity's phenyl side chains can still interact with opposite *Ln*MCs. The increased length of btDC separates opposite LaMC cavities by a greater distance. Thus the phenyl rings cannot interact with side-chains on opposite LaMCs and splay out instead. In addition to the size difference, the sulfur atoms on btDC make the anion more hydrophilic than naphDC. This introduces an energetic cost to burying the thiophene ring in the hydrophobic cavity, which contributes to the observed disruption. Lastly, **1** was crystallized from DMF while the naphDC structure was crystallized from a methanolic solution. DMF engages in critical interactions with the splayed out ligands of the disrupted cavity, further contributing to the vastly different structures obtained with the two guests.

*Ln*MC compartments with encapsulated guest complexes are described as clathratocomplexes [43, 82] because the complexes observed in the solid state do not persist in solution. Only 1 : 1 or 1 : 2 LaMC-guest complexes have been observed in solution by ESI-MS. However, dimeric and trimeric *Ln*MC species have recently been observed with nitrate guests in acetonitrile solutions [79]. Tegoni and coworkers suggested that the less donating solvent allowed the observation of the *Ln*MC aggregates. Given this observation, we analyzed **1** by ESI-MS from DMF solutions (Fig. S3, S4). It was necessary to add water to completely dissolve the solid. ESI-MS characterization revealed 2 : 2 host-guest complexes. The higher coordination number of La(III) is known to promote the inclusion of two guests in LaMCs, and compartments with multiple guests have been obtained in the solid state. However, no direct evidence of a LaMC dimer with two guests in solution has been reported. We feel that this dimer most likely contains two LaMCs bridged on their hydrophobic faces by two btDC guests. Though such a species is not directly observed in **1**, it serves as the most appropriate model considering that btDC would interact most favorably with the hydrophobic LaMC cavity.

Cavity disruption serendipitously led to the recognition of the less stable *cis*-HbtDC$^-$ rotamer. The large contact areas, limited volume, and shielding from reactive species afforded by molecular hosts is known to lead to the recognition of unstable guests [83 – 86], though this has never before been demonstrated with *Ln*MCs. *Ab-initio* calculations have determined that the *cis*-HbtDC rotamer is about 2 kJ mol^{-1} less stable than the *trans*-rotamer [69]. Despite the modest energy difference between the rotamers, this is novel demonstration of selectivity for *Ln*MCs. Analysis of **1** suggests that the stabilization of *cis*-HbtDC results from packing forces and not from the different geometries of the btDC rotamers. There is a 10.95 Å distance between the bound oxygen atoms on *cis*-btHDC$^-$. This distance could be realized with *trans*-btDC if its twist angle was between 145° and 176°. Therefore, the recognition of *cis*-HbtDC$^-$ is based on how it is packed and not on its size. Certainly the 2 kJ mol^{-1} energy difference can be overcome by packing forces.

Conclusion

The complex formed from LaMC and btDC displays features originating from in both rational design and serendipity. We utilized the design principle of *Ln*MC compartment disruption spurred by the inclusion of a long unsaturated dicarboxylate serendipitously to obtain a LaMC-btDC complex exhibiting no hydrophobic cavities. The structure consists of large

guest-bridged dimers that demonstrate the versatility of *Ln*MC clathratocomplexes through their expansive geometries, recognition of the less stable *cis*-HbtDC rotamer, and construction of nano-scale solvent channels. Additionally, direct evidence of LaMC dimerization in solution with btDC was obtained. Regarding efforts towards preparing functional crystalline solids through rational design, this structure suggests that guest length and solvent type promote the formation of close-packed assemblies of molecular compartments or open frameworks with significant void space from LaMC building blocks.

Experimental Section

*Preparation of **1***

Sodium hydroxide (0.16 g, 4 mmol) was dissolved in 5 mL of water. Bithiophene dicarboxylic acid [87] (0.26 g, 1.02 mmol) was dissolved in the solution. 10 mL of methanol was added, and the disodium salt was precipitated with 100 mL ether, filtered and air-dried. 15 mg of this light-yellow solid was added to $La(NO_3)_{2.5}[15\text{-}MC_{L-pheHA}\text{-}5](OH)_{0.5}(H_2O)_{3.5}$ (0.03 g, 0.018 mmol) dissolved in 8 mL of a 1 : 1 ethanol/water mixture. A precipitate quickly formed, which was filtered and dissolved in DMF. The solution was slowly evaporated to yield crystals with in one month. Yield: 11.2 mg (27 %). – ESI-MS (4 : 1 DMF/H_2O solution): *m/z* = 800.5 $[LaMC\text{-}btDC]^{2+}$, 837 $[LaMC\text{-}btDC\text{-}DMF]^{2+}$, 1600 $[LaMC\text{-}btDC]^{1+}$, $[LaMC_2\text{-}btDC_2]^{2+}$. – IR (KBr disk): ν = 3406, 1652, 1582, 1516, 1496, 1454, 1433, 1360, 1081, 1026, 776, 701, 593 cm^{-1}. – CHN analysis: calcd. C 39.75, H 5.26, N 9.65; found C 40.56, H 4.06, N 8.62.

X-Ray structure determination

A crystal of **1** with dimensions $0.35 \times 0.18 \times 0.08$ mm^3 was mounted on a standard Bruker SMART-APEX CCD-based X-ray diffractometer equipped with a low-temperature device and a fine focus Mo-target X-ray tube (λ = 0.71073 Å) operated at 1500 W power (50 kV, 30 mA). The X-ray intensities were measured at 85(2) K; the detector was placed 5.055 cm from the crystal. A total of 3730 frames were collected with a scan width of 0.5° in ω and 0.45° in ϕ and an exposure time of 60 s/frame. The frames were integrated with the Bruker SAINT software package [88] with a narrow frame algorithm. Data integration yielded a total of 203556 reflections to a maximum 2θ value of 56.66° of which 62188 were independent and 53539 were greater than $2\sigma(I)$. The final cell constants (Table 1) were based on the *xyz* centroids of 9185 reflections above $10\sigma(I)$. Analysis of the data showed negligible decay during data collection; the data were processed with SADABS [89] and corrected for absorption. The structure was solved and refined with the Bruker SHELXTL [90] (version 2008/4) software package. Several of the ligands are disordered over rotationally related sites. A number of lattice solvate molecules are also disordered. The model employed partially occupied atom sites and restraints to maintain chemical sensibility. Additional details are presented in Table 1. Table 2 summarizes selected bond lengths, angles, and dihedral angles for **1**, Tab. S1 additional bond lengths and angles.

CCDC 758963 contains the supplementary crystallographic data for this paper. These data can be obtained free of charge from The Cambridge Crystallographic Data Centre *via* www.ccdc.cam.ac.uk/data_request/cif.

Supporting Information

Additional figures of the *trans*-btDC- and *cis*-btDCH-bridged LaMC dimers, ESI-MS spectra, and a table with additional bond lengths and angles of **1** are provided as Supporting Information online only (http://www.znaturforsch.com/ab/v65b/c65b.htm).

Acknowledgement

The authors would like to thank the National Science Foundation for funding this work (CHE-0111428).

[1] C. J. Pedersen, *J. Am. Chem. Soc.* **1967**, *89*, 2495.
[2] C. J. Pedersen, *Science* **1988**, *241*, 536.
[3] J.-M. Lehn, *Angew. Chem.* **1988**, *100*, 1041; *Angew. Chem., Int. Ed. Engl.* **1988**, *27*, 89.
[4] D. J. Cram, *Angew. Chem.* **1988**, *100*, 1041; *Angew. Chem., Int. Ed. Engl.* **1988**, *27*, 1009.
[5] R. W. Saalfrank, H. Maid, A. Scheurer, *Angew. Chem.* **2008**, *120*, 8924; *Angew. Chem. Int. Ed.* **2008**, *47*, 8794.
[6] R. W. Saalfrank, N. Löw, S. Kareth, V. Seitz, F. Hampel, D. Stalke, M. Teichert, *Angew. Chem.* **1998**, *110*, 182; *Angew. Chem., Int. Ed. Engl.* **1998**, *37*, 172.
[7] O. Waldmann, J. Schülein, R. Koch, P. Müller, I. Bernt, R. W. Saalfrank, H. P. Andres, H. U. Güdel, P. Allenspach, *Inorg. Chem.* **1999**, *38*, 5879.
[8] R. W. Saalfrank, H. Maid, N. Mooren, F. Hampel, *Angew. Chem.* **2002**, *114*, 323; *Angew. Chem. Int. Ed.* **2002**, *41*, 304.
[9] R. W. Saalfrank, A. Dresel, V. Seitz, S. Trummer,

F. Hampel, M. Teichert, D. Stalke, C. Stadler, J. Daub, V. Schünemann, A. X. Trautwein, *Chem. Eur. J.* **1997**, *3*, 2058.
[10] R. W. Saalfrank, V. Seitz, D. L. Caulder, K. N. Raymond, M. Teichert, D. Stalke, *Eur. J. Inorg. Chem.* **1998**, 1313.
[11] M. S. Lah, B. R. Gibney, D. L. Tierney, J. E. Penner-Hahn, V. L. Pecoraro, *J. Am. Chem. Soc.* **1993**, *115*, 5857.
[12] C. Dendrinou-Samara, M. Alexiou, C. M. Zaleski, J. W. Kampf, M. L. Kirk, D. P. Kessissoglou, V. L. Pecoraro, *Angew. Chem.* **2003**, *115*, 3893; *Angew. Chem. Int. Ed.* **2003**, *42*, 3763.
[13] V. L. Pecoraro, *Inorg. Chim. Acta* **1989**, *155*, 171.
[14] B. R. Gibney, A. J. Stemmler, S. Pilotek, J. W. Kampf, V. L. Pecoraro, *Inorg. Chem.* **1993**, *32*, 6008.
[15] M. S. Lah, M. L. Kirk, W. Hatfield, V. L. Pecoraro, *J. Chem. Soc., Chem. Comm.* **1989**, 1606.
[16] M. S. Lah, V. L. Pecoraro, *J. Am. Chem. Soc.* **1989**, *111*, 7258.
[17] M. S. Lah, V. L. Pecoraro, *Comments Inorg. Chem.* **1990**, *11*, 59.
[18] M. S. Lah, V. L. Pecoraro, *Inorg. Chem.* **1991**, *30*, 878.
[19] V. L. Pecoraro, A. J. Stemmler, B. R. Gibney, J. J. Bodwin, H. Wang, J. W. Kampf, A. Barwinski in *Prog. Inorg. Chem.*, Vol. 45 (ed.: K. D. Karlin), John Wiley and Sons, Inc., New York, **1997**, pp. 83.
[20] G. Mezei, C. M. Zaleski, V. L. Pecoraro, *Chem. Rev.* **2007**, *107*, 4933.
[21] A. Caneschi, A. Cornia, S. J. Lippard, *Angew. Chem.* **1995**, *107*, 511; *Angew. Chem., Int. Ed. Engl.* **1995**, *34*, 467.
[22] M. Tegoni, L. Ferretti, F. Sansone, M. Remelli, V. Bertolasi, F. Dallavalle, *Chem. Eur. J.* **2007**, *13*, 1300.
[23] R. W. Saalfrank, N. Löw, F. Hampel, H. Stachel, *Angew. Chem.* **1996**, *108*, 2353; *Angew. Chem., Int. Ed. Engl.* **1996**, *35*, 2209.
[24] C. M. Zaleski, E. C. Depperman, J. W. Kampf, M. L. Kirk, V. L. Pecoraro, *Angew. Chem.* **2004**, *116*, 4002; *Angew. Chem. Int. Ed.* **2004**, *43*, 3912.
[25] C. M. Zaleski, E. C. Depperman, C. Dendrinou-Samara, M. Alexiou, J. W. Kampf, D. P. Kessissoglou, M. L. Kirk, V. L. Pecoraro, *J. Am. Chem. Soc.* **2005**, *127*, 12862.
[26] O. Waldmann, R. Koch, S. Schromm, J. Schülein, P. Müller, I. Bernt, R. W. Saalfrank, F. Hampel, E. Balthes, *Inorg. Chem.* **2001**, *40*, 2986.
[27] R. W. Saalfrank, A. Scheurer, I. Bernt, F. W. Heinemann, A. V. Postnikov, V. Schünemann, A. X. Trautwein, M. S. Alam, H. Rupp, P. Müller, *J. Chem. Soc., Dalton Trans.* **2006**, 2865.
[28] H. Andres, R. Basler, A. J. Blake, C. Cadiou, G. Chaboussant, C. M. Grant, H.-U. Güdel, M. Murrie, S. Parsons, C. Paulsen, F. Semadini, V. Villar, W. Wernsdorfer, R. E. P. Winpenny, *Chem. Eur. J.* **2002**, *8*, 4867.
[29] M. Affronte, S. Carretta, G. A. Timco, R. E. P. Winpenny, *Chem. Commun.* **2007**, 1789.
[30] S. Piligkos, H. Weihe, E. Bill, F. Neese, H. El Mkami, G. M. Smith, D. Collison, G. Rajaraman, G. A. Timco, R. E. P. Winpenny, E. J. L. McInnes, *Chem. Eur. J.* **2009**, *15*, 3152.
[31] C. Dendrinou-Samara, G. Psomas, L. Iordanidis, V. Tangoulis, D. P. Kessissoglou, *Chem. Eur. J.* **2001**, *7*, 5041.
[32] G. Psomas, A. J. Stemmler, C. Dendrinou-Samara, J. J. Bodwin, M. Scheider, M. Alexiou, J. W. Kampf, D. P. Kessissoglou, V. L. Pecoraro, *Inorg. Chem.* **2001**, *40*, 1562.
[33] A. J. Stemmler, J. W. Kampf, V. L. Pecoraro, *Inorg. Chem.* **1995**, *34*, 2271.
[34] G. Psomas, C. Dendrinou-Samara, M. Alexiou, A. Tsohos, C. P. Raptopoulou, A. Terzis, D. P. Kessissoglou, *Inorg. Chem.* **1998**, *37*, 6556.
[35] B. R. Gibney, H. Wang, J. W. Kampf, V. L. Pecoraro, *Inorg. Chem.* **1996**, *35*, 6184.
[36] J. A. Halfen, J. J. Bodwin, V. L. Pecoraro, *Inorg. Chem.* **1998**, *37*, 5416.
[37] C. Dendrinou-Samara, L. Alevizopoulou, L. Iordanidis, E. Samaras, D. P. Kessissoglou, *J. Inorg. Biochem.* **2002**, *89*, 89.
[38] R. H. Laye, F. K. Larsen, J. Overgaard, C. A. Muryn, E. J. L. McInnes, E. Rentschler, V. Sanchez, S. J. Teat, H.-U. Güdel, O. Waldmann, G. A. Timco, R. E. P. Winpenny, *Chem. Commun.* **2005**, 1125.
[39] R. W. Saalfrank, C. Deutscher, S. Sperner, K. Nakajima, A. M. Ako, E. Uller, F. Hampel, F. W. Heinemann, *Inorg. Chem.* **2004**, *43*, 4372.
[40] R. W. Saalfrank, E. Uller, B. Demleitner, I. Bernt, *Struct. Bonding* **2000**, *96*, 149.
[41] M. Moon, I. Kim, M. S. Lah, *Inorg. Chem.* **2000**, *39*, 2710.
[42] J. J. Bodwin, V. L. Pecoraro, *Inorg. Chem.* **2000**, *39*, 3434.
[43] G. Mezei, J. W. Kampf, S. Pan, K. R. Poeppelmeier, B. Watkins, V. L. Pecoraro, *Chem. Commun.* **2007**, *11*, 1148.
[44] C. S. Lim, J. Jankolovits, J. W. Kampf, V. L. Pecoraro, *Chem. Asian. J.* **2010**, *5*, 46.
[45] D. P. Kessissoglou, J. W. Kampf, V. L. Pecoraro, *Polyhedron* **1994**, *13*, 1379.
[46] A. J. Stemmler, J. W. Kampf, V. L. Pecoraro, *Angew. Chem.* **1996**, *108*, 3011; *Angew. Chem., Int. Ed. Engl.* **1996**, *35*, 2841.
[47] V. L. Pecoraro, J. J. Bodwin, A. D. Cutland, *J. Solid State Chem.* **2000**, *152*, 68.
[48] A. J. Stemmler, A. Barwinski, M. J. Baldwin, V. Young,

V. L. Pecoraro, *J. Am. Chem. Soc.* **1996**, *118*, 11962.
[49] A. J. Stemmler, J. W. Kampf, M. L. Kirk, B. H. Atasi, V. L. Pecoraro, *Inorg. Chem.* **1999**, *38*, 2807.
[50] T. N. Parac-Vogt, A. Pacco, C. Görller-Walrand, K. Binnemans, *J. Inorg. Biochem.* **2005**, *99*, 497.
[51] C. M. Zaleski, E. C. Depperman, J. W. Kampf, M. L. Kirk, V. L. Pecoraro, *Inorg. Chem.* **2006**, *45*, 10022.
[52] J. J. Bodwin, A. D. Cutland, R. G. Malkani, V. L. Pecoraro, *Coord. Chem. Rev.* **2001**, *216 – 217*, 489.
[53] A. D. Cutland, R. G. Malkani, J. W. Kampf, V. L. Pecoraro, *Angew. Chem.* **2000**, *112*, 2801; *Angew. Chem. Int. Ed.* **2000**, *39*, 2689.
[54] C.-S. Lim, J. W. Kampf, V. L. Pecoraro, *Inorg. Chem.* **2009**, *48*, 5224.
[55] M. Tegoni, M. Tropiano, L. Marchio, *J. Chem. Soc., Dalton Trans.* **2009**, 6705.
[56] A. C. Cutland-Van Noord, J. W. Kampf, V. L. Pecoraro, *Angew. Chem.* **2002**, *114*, 4861; *Angew. Chem. Int. Ed.* **2002**, *41*, 4667.
[57] C. M. Zaleski, A. D. Cutland-Van Noord, J. W. Kampf, V. L. Pecoraro, *Cryst. Growth Des.* **2007**, *7*, 1098.
[58] J. A. Johnson, J. W. Kampf, V. L. Pecoraro, *Angew. Chem.* **2003**, *115*, 564; *Angew. Chem. Int. Ed.* **2003**, *42*, 546.
[59] A. D. Cutland, J. A. Halfen, J. W. Kampf, V. L. Pecoraro, *J. Am. Chem. Soc.* **2001**, *123*, 6211.
[60] C.-S. Lim, A. C. V. Noord, J. W. Kampf, V. L. Pecoraro, *Eur. J. Inorg. Chem.* **2007**, 1347.
[61] W. J. Evans, B. L. Davis, G. W. Nyce, J. M. Perotti, J. W. Ziller, *J. Organomet. Chem.* **2003**, *677*, 89.
[62] H. C. Aspinall, J. Black, I. Dodd, M. M. Harding, S. J. Winkley, *J. Chem. Soc., Dalton Trans.* **1993**, 709.
[63] L. Natrajan, J. Pecaut, M. Mazzanti, *J. Chem. Soc., Dalton Trans.* **2006**, 1002.
[64] O. A. Gerasko, E. A. Mainicheva, M. I. Naumova, M. Neumaier, M. M. Kappes, S. Lebedkin, D. Fenske, V. P. Fedin, *Inorg. Chem.* **2008**, *47*, 8869.
[65] C. Runschke, G. Meyer, *Z. Anorg. Allg. Chem.* **1997**, *623*, 1493.
[66] C. A. Hunter, J. K. M. Sanders, *J. Am. Chem. Soc.* **1990**, *112*, 5525.
[67] J. C. Ma, D. A. Dougherty, *Chem. Rev.* **1997**, *97*, 1303.
[68] J. E. Chadwick, B. E. Kohler, *J. Phys. Chem.* **1994**, *98*, 3631.
[69] E. Orti, P. M. Viruela, J. Sanchez-Marin, F. Tomas, *J. Phys. Chem.* **1995**, *99*, 4955.
[70] A. M. Fedor, D. G. Allis, T. M. Korter, *Vib. Spectrosc.* **2009**, *49*, 124.
[71] G. Barbarella, M. Zambianchi, A. Bongnini, L. Antolini, *Adv. Mater.* **1993**, *5*, 834.
[72] P. A. Chalconer, S. R. Gunatunga, P. B. Hitchcock, *J. Chem. Soc., Perkin Trans.* **1997**, *2*, 1597.
[73] H. Muguruma, K. Kobiro, S. Hotta, *Chem. Mater.* **1998**, *10*, 1459.
[74] D. B. Mitzi, K. Chondroudis, C. R. Kagan, *Inorg. Chem.* **1999**, *38*, 6246.
[75] D. B. Mitzi, *Inorg. Chem.* **2000**, *39*, 6107.
[76] M. M. Bader, R. Custelcean, M. D. Ward, *Chem. Mater.* **2003**, *15*, 616.
[77] D. M. Kang, S. G. Kim, S. J. Lee, J. K. Park, K. M. Park, S. C. Shin, *Bull. Korean Chem. Soc.* **2005**, *26*, 1390.
[78] A. L. Spek, PLATON, A Multipurpose Crystallographic Tool, Utrecht University, Utrecht (The Netherlands) **2001**. See also: A. L. Spek, *J. Appl. Crystallogr.* **2003**, *36*, 7.
[79] F. Dallavalle, M. Remelli, F. Sansone, D. Bacco, M. Tegoni, *Inorg. Chem.* **2010**, *49*. 1761.
[80] H. Li, M. Eddaoudi, M. O'Keeffe, O. M. Yaghi, *Nature* **1999**, *402*, 276.
[81] J. D. Wuest, *Chem. Commun.* **2005**, 5830.
[82] E. Weber, H.-P. Josel, *J. Inclusion Phenom.* **1983**, *1*, 79.
[83] D. J. Cram, M. E. Tanner, R. Thomas, *Angew. Chem.* **1991**, *103*, 1048; *Angew. Chem., Int. Ed. Eng.* **1991**, *30*, 1024.
[84] S. K. Korner, F. C. Tucci, D. M. Rudkevich, T. Heinz, J. Rebek, Jr., *Chem. Eur. J.* **2000**, *6*, 187.
[85] M. D. Pluth, R. G. Bergman, K. N. Raymond, *Acc. Chem. Res.* **2009**, *42*, 1650.
[86] P. Mal, B. Breiner, K. Rissanen, J. R. Nitschke, *Science* **2009**, *324*, 1697.
[87] H. Wynberg, A. Bantjes, *J. Am. Chem. Soc.* **1960**, *82*, 1447.
[88] SAINT+ (version 7.60A), Bruker Analytical X-ray Instruments Inc., Madison, Wisconsin (USA) **2009**.
[89] G. M. Sheldrick, SADABS (version 2008/1), Program for Empirical Absorption Correction of Area Detector Data, University of Göttingen, Göttingen (Germany) **2008**.
[90] G. M. Sheldrick, SHELXTL (version 2008/4), Bruker Analytical X-ray Instruments Inc., Madison, Wisconsin (USA) **2008**. See also: G. M. Sheldrick, *Acta Crystallogr.* **2008**, *A64*, 112.

Disruption of the La(III)[15-Metallacrown-5] Cavity through Bithiophene Dicarboxylate Inclusion

Joseph Jankolovits, Choong-Sun Lim, Jeff W. Kampf, and Vincent L. Pecoraro

Department of Chemistry, Willard H. Dow Laboratories, The University of Michigan, Ann Arbor, MI 48109-1055, USA

Supporting Information

Fig. S1. Image of the *trans*-btDC bridged LaMC dimer that displays some of the atom labels used in the dihedral angles for section 2. The btDC guest with the sulfur labels S_3 and S_4 is disordered with a btDC that possesses a different dihedral angle. That guest is not show to enhance the clarity of the image. Color scheme: grey - carbon, yellow - sulfur, red - oxygen, blue - nitrogen, orange - copper, light blue - lanthanum.

Fig. S2. Image of the *cis*-btDCH bridged LaMC dimer that displays some of the atom labels used in the dihedral angles for section 2. Color scheme: grey - carbon, yellow - sulfur, red - oxygen, blue - nitrogen, orange - copper, light blue - lanthanum.

Fig. S3. ESI-MS spectrum of **1** in a 4:1 DMF/water solution.

Fig. S4. Selected portion of the ESI-MS spectrum of **1** displaying the peaks corresponding to a 2:2 LaMC-btDC^{2+} ion.

Table S1. Bond lengths [A] and angles [deg] for **1**. The labeling scheme corresponds to the labels from the cif file for **1** and not the labels used in Table 2 or Figures 4, S1, S2.

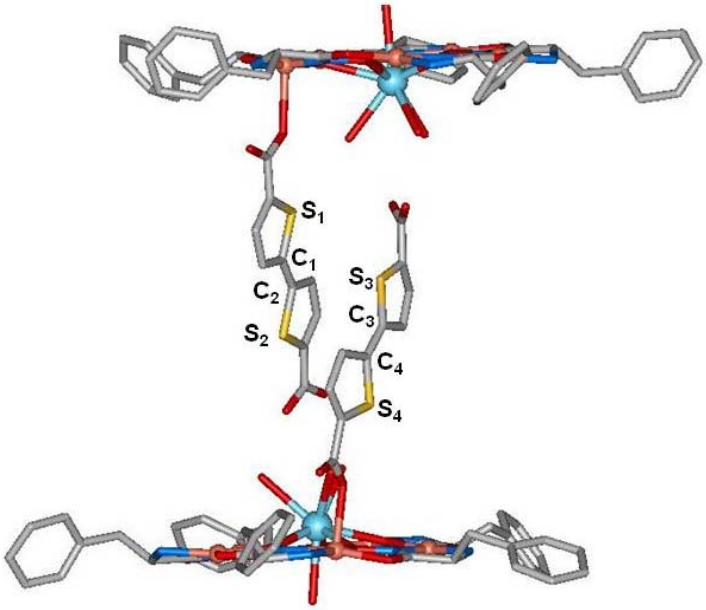

Fig. S1. Image of the *trans*-btDC bridged LaMC dimer that displays some of the atom labels used in the dihedral angles for section 2. The btDC guest with the sulfur labels S_3 and S_4 is disordered with a btDC that possesses a different dihedral angle. That guest is not show to enhance the clarity of the image. Color scheme: grey - carbon, yellow - sulfur, red - oxygen, blue - nitrogen, orange - copper, light blue - lanthanum.

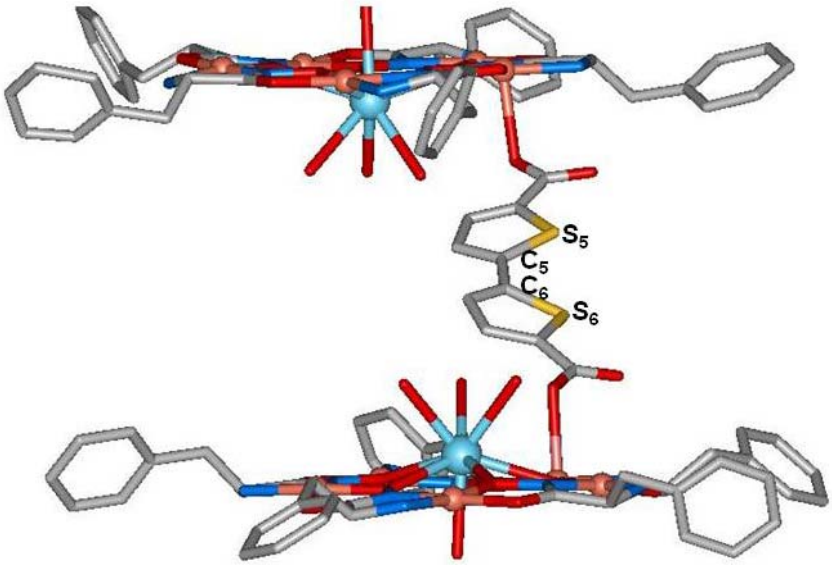

Fig. S2. Image of the *cis*-btDCH bridged LaMC dimer that displays some of the atom labels used in the dihedral angles for section 2. Color scheme: grey - carbon, yellow - sulfur, red - oxygen, blue - nitrogen, orange - copper, light blue - lanthanum.

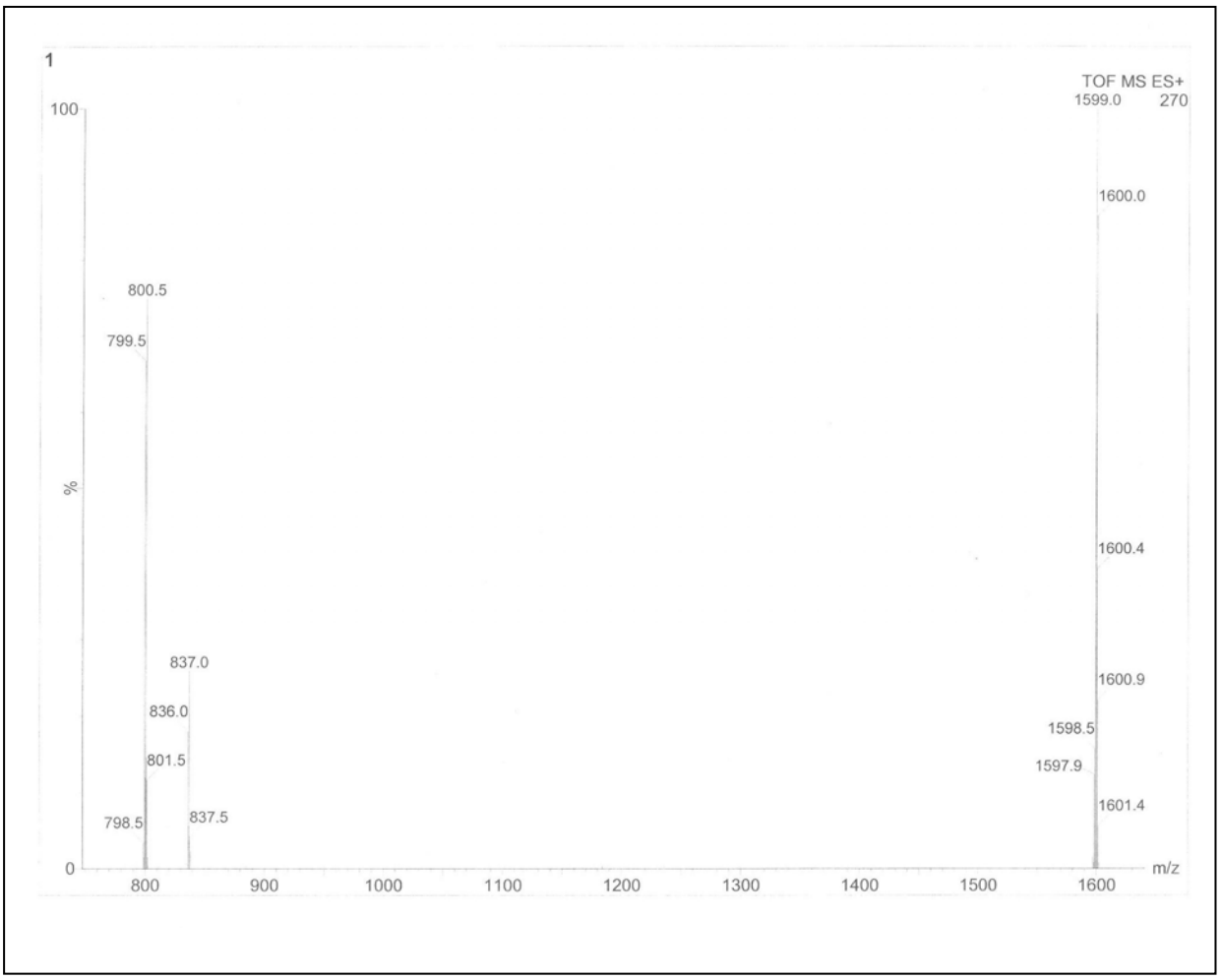

Fig. S3. ESI-MS spectrum of **1** in a 4:1 DMF/water solution.

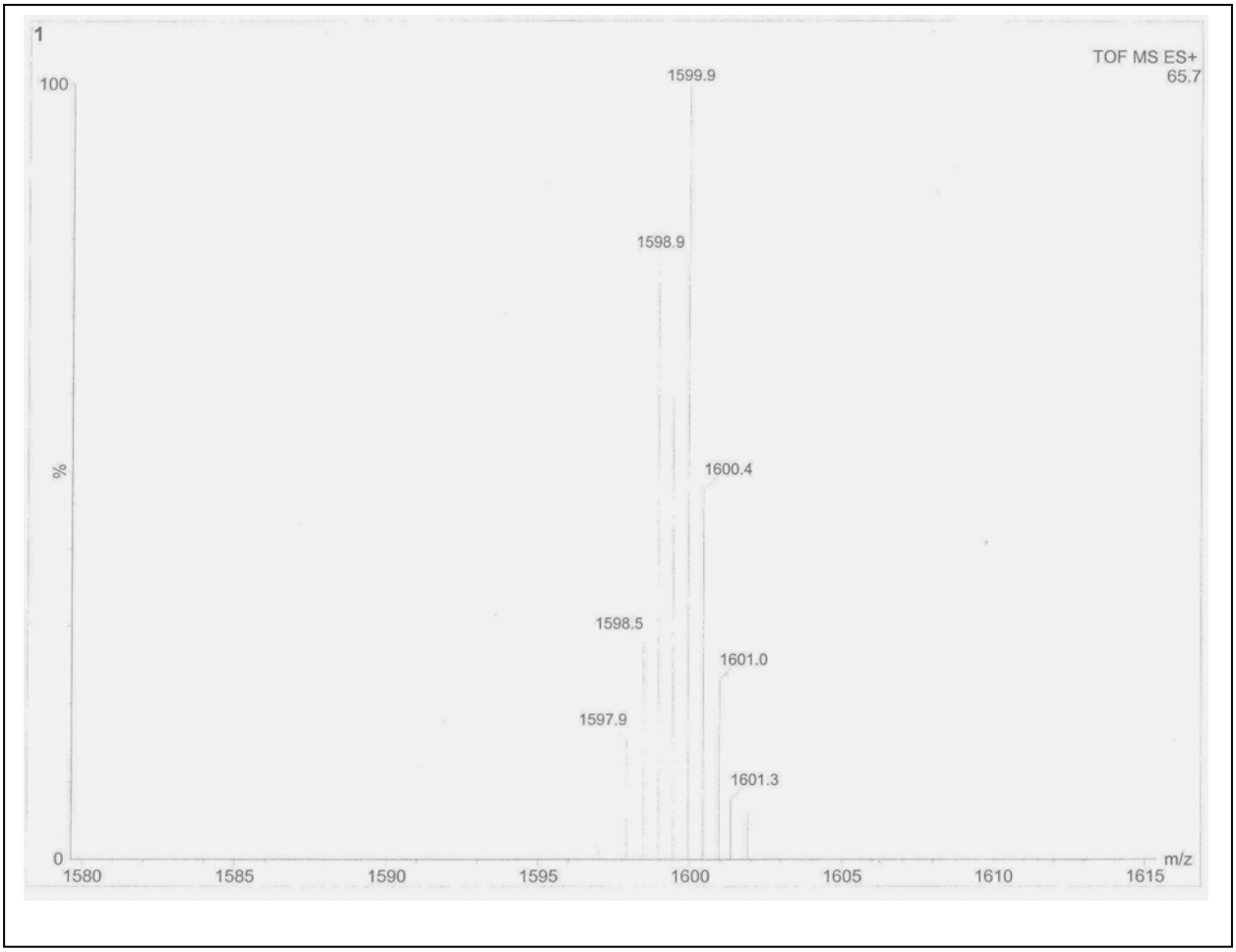

Fig. S4. Selected portion of the ESI-MS spectrum of **1** displaying the peaks corresponding to a 2:2 LaMC-btDC^{2+} ion.

Table S1. Bond lengths [A] and angles [deg] for **1**. The labeling scheme corresponds to the labels from the cif file for **1** and not the labels used in Table 2 or Figures 4, S1, S2.

La(1)-O(350)	2.500(2)
La(1)-O(351)	2.5249(18)
La(1)-O(14)	2.5547(17)
La(1)-O(18)	2.5552(15)
La(1)-O(20)	2.5574(15)
La(1)-O(12)	2.558(2)
La(1)-O(352)	2.574(2)
La(1)-O(16)	2.5793(18)
La(1)-O(353)	2.617(2)
La(2)-O(355)	2.5062(18)
La(2)-O(4)	2.5422(17)
La(2)-O(356)	2.5506(15)
La(2)-O(10)	2.5588(14)
La(2)-O(2)	2.5625(16)
La(2)-O(354)	2.5708(18)
La(2)-O(6)	2.5715(15)
La(2)-O(8)	2.5827(18)
La(2)-O(353)	2.6241(19)
Cu(1)-N(10)	1.902(2)
Cu(1)-O(2)	1.9276(15)
Cu(1)-O(1)	1.963(2)
Cu(1)-N(9)	2.008(2)

Cu(1)-O(200)	2.3583(17)
Cu(2)-N(2)	1.8800(18)
Cu(2)-O(4)	1.9016(18)
Cu(2)-O(3)	1.9330(15)
Cu(2)-N(1)	2.001(2)
Cu(3)-O(6)	1.9081(15)
Cu(3)-N(4)	1.908(2)
Cu(3)-O(5)	1.9382(18)
Cu(3)-N(3)	2.010(2)
Cu(4)-N(6)	1.896(2)
Cu(4)-O(8)	1.9293(16)
Cu(4)-O(7)	1.9500(18)
Cu(4)-N(5)	2.011(2)
Cu(5)-N(8)	1.8923(19)
Cu(5)-O(10)	1.9062(19)
Cu(5)-O(9)	1.9375(17)
Cu(5)-N(7)	2.010(2)
Cu(6)-N(20)	1.894(2)
Cu(6)-O(12)	1.9049(19)
Cu(6)-O(11)	1.941(2)
Cu(6)-N(19)	2.008(2)
Cu(7)-N(18)	1.900(2)
Cu(7)-O(20)	1.9223(16)
Cu(7)-O(19)	1.9516(19)
Cu(7)-N(17)	2.009(2)

Cu(7)-O(302)	2.4186(18)
Cu(8)-N(16)	1.8848(17)
Cu(8)-O(18)	1.9117(18)
Cu(8)-O(17)	1.9302(14)
Cu(8)-N(15)	2.026(2)
Cu(9)-N(14)	1.899(2)
Cu(9)-O(16)	1.9242(15)
Cu(9)-O(15)	1.9568(17)
Cu(9)-N(13)	2.0080(19)
Cu(9)-O(250)	2.4162(14)
Cu(10)-O(14)	1.9044(18)
Cu(10)-N(12)	1.909(2)
Cu(10)-O(13)	1.9265(19)
Cu(10)-N(11)	1.994(3)
S(1)-C(301)	1.736(3)
S(1)-C(304)	1.743(3)
S(2)-C(305)	1.699(3)
S(2)-C(308)	1.732(3)
O(1)-C(1)	1.291(3)
O(2)-N(2)	1.400(3)
O(3)-C(10)	1.295(3)
O(4)-N(4)	1.405(2)
O(5)-C(19)	1.301(3)
O(6)-N(6)	1.399(3)
O(7)-C(28)	1.287(3)

O(8)-N(8)	1.400(2)
O(9)-C(37)	1.304(4)
O(10)-N(10)	1.387(3)
O(11)-C(46)	1.298(3)
O(12)-N(12)	1.374(3)
O(13)-C(55)	1.305(3)
O(14)-N(14)	1.408(3)
O(15)-C(64)	1.290(2)
O(16)-N(16)	1.392(3)
O(17)-C(73)	1.315(3)
O(18)-N(18)	1.394(2)
O(19)-C(82)	1.280(3)
O(20)-N(20)	1.396(3)
N(1)-C(2)	1.479(3)
N(2)-C(1)	1.320(3)
N(3)-C(11)	1.479(3)
N(4)-C(10)	1.300(3)
N(5)-C(20)	1.480(3)
N(6)-C(19)	1.313(3)
N(7)-C(29)	1.482(4)
N(8)-C(28)	1.321(3)
N(9)-C(38)	1.479(4)
N(10)-C(37)	1.316(3)
N(11)-C(47)	1.495(4)
N(12)-C(46)	1.306(4)

N(13)-C(56)	1.473(3)
N(14)-C(55)	1.303(3)
N(15)-C(65)	1.474(3)
N(16)-C(64)	1.325(3)
N(17)-C(74)	1.470(4)
N(18)-C(73)	1.295(3)
N(19)-C(83)	1.477(3)
N(20)-C(82)	1.310(3)
C(1)-C(2)	1.497(4)
C(2)-C(3)	1.551(4)
C(3)-C(0A)	1.471(7)
C(3)-C(4)	1.541(4)
C(4)-C(9)	1.367(4)
C(4)-C(5)	1.418(4)
C(5)-C(6)	1.395(6)
C(6)-C(7)	1.403(5)
C(7)-C(8)	1.375(5)
C(8)-C(9)	1.397(6)
C(0A)-C(0F)	1.363(7)
C(0A)-C(0B)	1.381(6)
C(0B)-C(0C)	1.405(9)
C(0C)-C(0D)	1.381(8)
C(0D)-C(0E)	1.372(7)
C(0E)-C(0F)	1.391(9)
C(10)-C(11)	1.522(3)

C(11)-C(12)	1.528(3)
C(12)-C(13)	1.525(3)
C(13)-C(18)	1.386(3)
C(13)-C(14)	1.397(4)
C(14)-C(15)	1.392(4)
C(15)-C(16)	1.397(4)
C(16)-C(17)	1.348(5)
C(17)-C(18)	1.395(5)
C(19)-C(20)	1.510(4)
C(20)-C(21)	1.540(3)
C(21)-C(22)	1.498(4)
C(22)-C(27)	1.384(4)
C(22)-C(23)	1.385(5)
C(23)-C(24)	1.392(5)
C(24)-C(25)	1.410(5)
C(25)-C(26)	1.362(6)
C(26)-C(27)	1.399(5)
C(28)-C(29)	1.518(3)
C(29)-C(30)	1.539(4)
C(30)-C(31)	1.538(4)
C(31)-C(32)	1.347(5)
C(31)-C(36)	1.396(7)
C(32)-C(33)	1.388(6)
C(33)-C(34)	1.313(8)
C(34)-C(35)	1.310(9)

C(35)-C(36)	1.451(8)
C(37)-C(38)	1.508(3)
C(38)-C(39)	1.527(4)
C(39)-C(40)	1.517(4)
C(40)-C(45)	1.383(5)
C(40)-C(41)	1.386(3)
C(41)-C(42)	1.392(4)
C(42)-C(43)	1.398(5)
C(43)-C(44)	1.379(4)
C(44)-C(45)	1.406(5)
C(46)-C(47)	1.510(4)
C(47)-C(48)	1.508(4)
C(48)-C(5A)	1.478(6)
C(48)-C(49)	1.513(5)
C(49)-C(54)	1.400(7)
C(49)-C(50)	1.404(6)
C(50)-C(51)	1.398(7)
C(51)-C(52)	1.375(9)
C(52)-C(53)	1.383(7)
C(53)-C(54)	1.377(8)
C(5A)-C(5F)	1.385(7)
C(5A)-C(5B)	1.404(8)
C(5B)-C(5C)	1.416(8)
C(5C)-C(5D)	1.375(8)
C(5D)-C(5E)	1.377(9)

C(5E)-C(5F)	1.381(8)
C(55)-C(56)	1.525(4)
C(56)-C(57)	1.553(3)
C(57)-C(58)	1.508(5)
C(58)-C(63)	1.366(5)
C(58)-C(59)	1.399(5)
C(59)-C(60)	1.392(6)
C(60)-C(61)	1.327(6)
C(61)-C(62)	1.411(6)
C(62)-C(63)	1.380(6)
C(64)-C(65)	1.513(3)
C(65)-C(66)	1.533(3)
C(66)-C(67)	1.482(4)
C(67)-C(68)	1.390(4)
C(67)-C(72)	1.400(4)
C(68)-C(69)	1.411(5)
C(69)-C(70)	1.372(6)
C(70)-C(71)	1.377(6)
C(71)-C(72)	1.367(5)
C(73)-C(74)	1.500(3)
C(74)-C(7G)	1.549(5)
C(74)-C(75)	1.550(5)
C(82)-C(83)	1.503(4)
C(83)-C(84)	1.549(4)
C(84)-C(85)	1.522(5)

C(85)-C(86)	1.348(5)
C(85)-C(90)	1.424(4)
C(86)-C(87)	1.392(8)
C(87)-C(88)	1.345(5)
C(88)-C(89)	1.346(6)
C(89)-C(90)	1.415(6)
O(200)-C(200)	1.261(6)
O(200)-C(20A)	1.290(6)
O(201)-C(200)	1.271(6)
C(200)-C(201)	1.507(7)
C(201)-C(202)	1.368(10)
C(201)-S(3)	1.672(5)
C(202)-C(203)	1.402(8)
C(203)-C(204)	1.477(9)
C(204)-C(205)	1.432(5)
C(204)-S(3)	1.739(5)
S(4)-C(205)	1.723(5)
S(4)-C(208)	1.784(5)
C(205)-C(206)	1.294(6)
C(206)-C(207)	1.416(7)
C(207)-C(208)	1.225(10)
C(208)-C(209)	1.456(6)
C(209)-O(203)	1.245(6)
C(209)-O(202)	1.263(6)
O(215)-C(215)	1.226(7)

N(215)-C(215)	1.354(9)
N(215)-C(216)	1.432(8)
N(215)-C(217)	1.518(10)
C(75)-C(76)	1.519(6)
C(76)-C(77)	1.378(7)
C(76)-C(81)	1.393(8)
C(77)-C(78)	1.415(9)
C(78)-C(79)	1.357(9)
C(79)-C(80)	1.360(7)
C(80)-C(81)	1.380(8)
O(20A)-C(20A)	1.261(5)
C(20A)-C(20B)	1.510(6)
C(20B)-C(20C)	1.366(9)
C(20B)-S(3A)	1.762(4)
C(20C)-C(20D)	1.429(6)
C(20D)-C(20E)	1.405(8)
C(20E)-C(20F)	1.441(5)
C(20E)-S(3A)	1.710(5)
S(4A)-C(20F)	1.733(5)
S(4A)-C(20I)	1.759(5)
C(20F)-C(20G)	1.496(8)
C(20G)-C(20H)	1.367(6)
C(20H)-C(20I)	1.314(9)
C(20I)-C(20J)	1.462(6)
C(20J)-O(20C)	1.225(6)

C(20J)-O(20B)	1.236(7)
O(21A)-C(21A)	1.173(9)
C(21A)-N(21A)	1.303(11)
N(21A)-C(21B)	1.474(8)
N(21A)-C(21C)	1.477(7)
C(7G)-C(7A)	1.519(4)
C(7A)-C(7B)	1.391(6)
C(7A)-C(7F)	1.398(6)
C(7B)-C(7C)	1.411(6)
C(7C)-C(7D)	1.402(7)
C(7D)-C(7E)	1.367(7)
C(7E)-C(7F)	1.365(5)
O(250)-C(250)	1.267(2)
O(251)-C(250)	1.248(3)
C(250)-C(251)	1.502(3)
C(251)-C(252)	1.357(3)
C(251)-S(5)	1.726(2)
C(252)-C(253)	1.398(5)
C(253)-C(254)	1.344(4)
C(254)-C(255)	1.459(4)
C(254)-S(5)	1.7347(19)
S(6)-C(258)	1.713(3)
S(6)-C(255)	1.7244(19)
C(255)-C(256)	1.353(3)
C(256)-C(257)	1.410(4)

C(257)-C(258)	1.354(3)
C(258)-C(259)	1.464(3)
C(259)-O(252)	1.245(4)
C(259)-O(253)	1.268(3)
O(300)-C(300)	1.280(4)
O(301)-C(300)	1.241(4)
O(302)-C(309)	1.278(4)
O(303)-C(309)	1.232(4)
C(300)-C(301)	1.501(4)
C(301)-C(302)	1.362(5)
C(302)-C(303)	1.428(5)
C(303)-C(304)	1.356(5)
C(304)-C(305)	1.463(4)
C(305)-C(306)	1.394(5)
C(306)-C(307)	1.457(6)
C(307)-C(308)	1.296(5)
C(308)-C(309)	1.530(5)
O(420)-C(420)	1.235(11)
C(420)-N(420)	1.324(7)
N(420)-C(421)	1.387(9)
N(420)-C(422)	1.489(10)
O(423)-C(423)	1.225(10)
C(423)-N(423)	1.323(8)
N(423)-C(424)	1.425(9)
N(423)-C(425)	1.454(8)

O(427)-C(427)	1.233(10)
C(427)-N(427)	1.337(6)
N(427)-C(428)	1.431(9)
N(427)-C(429)	1.458(9)
O(500)-C(500)	1.163(4)
C(500)-N(500)	1.378(6)
N(500)-C(501)	1.451(7)
N(500)-C(502)	1.501(7)
O(50A)-C(50A)	1.518(14)
C(50A)-C(50B)	1.507(16)
O(505)-C(505)	1.377(7)
N(505)-C(505)	1.387(5)
N(505)-C(507)	1.453(8)
N(505)-C(506)	1.549(8)
O(515)-C(515)	1.241(4)
N(515)-C(515)	1.365(5)
N(515)-C(516)	1.402(4)
N(515)-C(517)	1.457(5)
O(525)-C(525)	1.228(10)
N(525)-C(525)	1.283(8)
N(525)-C(526)	1.423(6)
N(525)-C(527)	1.482(9)
O(530)-C(530)	1.272(9)
N(530)-C(530)	1.289(8)
N(530)-C(531)	1.461(8)

N(530)-C(532)	1.468(8)
O(540)-C(540)	1.231(4)
N(540)-C(540)	1.311(4)
N(540)-C(541)	1.409(5)
N(540)-C(542)	1.461(5)
O(550)-C(550)	1.272(5)
N(550)-C(550)	1.352(6)
N(550)-C(551)	1.388(6)
N(550)-C(552)	1.473(5)
O(560)-C(560)	1.243(6)
N(560)-C(560)	1.342(5)
N(560)-C(562)	1.394(5)
N(560)-C(561)	1.419(8)
O(570)-C(570)	1.226(5)
C(570)-N(570)	1.321(6)
N(570)-C(571)	1.428(5)
N(570)-C(572)	1.434(5)
O(590)-C(590)	1.240(4)
N(590)-C(590)	1.342(3)
N(590)-C(592)	1.452(5)
N(590)-C(591)	1.470(5)
O(603)-O(60Y)	1.127(10)
O(70A)-C(70A)	1.200(10)
C(70A)-N(70A)	1.341(8)
N(70A)-C(70B)	1.419(7)

N(70A)-C(70C)	1.472(8)

O(350)-La(1)-O(351)	69.54(7)
O(350)-La(1)-O(14)	143.64(6)
O(351)-La(1)-O(14)	92.72(6)
O(350)-La(1)-O(18)	84.71(7)
O(351)-La(1)-O(18)	91.89(6)
O(14)-La(1)-O(18)	128.73(5)
O(350)-La(1)-O(20)	70.95(6)
O(351)-La(1)-O(20)	137.20(6)
O(14)-La(1)-O(20)	129.48(5)
O(18)-La(1)-O(20)	68.62(5)
O(350)-La(1)-O(12)	102.55(8)
O(351)-La(1)-O(12)	137.20(6)
O(14)-La(1)-O(12)	68.64(6)
O(18)-La(1)-O(12)	130.15(4)
O(20)-La(1)-O(12)	67.73(5)
O(350)-La(1)-O(352)	68.46(8)
O(351)-La(1)-O(352)	70.72(9)
O(14)-La(1)-O(352)	75.83(7)
O(18)-La(1)-O(352)	151.64(7)
O(20)-La(1)-O(352)	108.81(8)
O(12)-La(1)-O(352)	67.51(8)
O(350)-La(1)-O(16)	127.22(7)
O(351)-La(1)-O(16)	67.83(5)

O(14)-La(1)-O(16)	67.60(6)
O(18)-La(1)-O(16)	67.27(5)
O(20)-La(1)-O(16)	129.23(5)
O(12)-La(1)-O(16)	129.90(6)
O(352)-La(1)-O(16)	121.95(8)
O(350)-La(1)-O(353)	143.92(7)
O(351)-La(1)-O(353)	137.88(8)
O(14)-La(1)-O(353)	69.33(6)
O(18)-La(1)-O(353)	73.51(6)
O(20)-La(1)-O(353)	74.40(7)
O(12)-La(1)-O(353)	72.64(7)
O(352)-La(1)-O(353)	134.24(8)
O(16)-La(1)-O(353)	70.10(7)
O(355)-La(2)-O(4)	97.60(6)
O(355)-La(2)-O(356)	69.96(6)
O(4)-La(2)-O(356)	74.34(6)
O(355)-La(2)-O(10)	83.05(5)
O(4)-La(2)-O(10)	133.17(5)
O(356)-La(2)-O(10)	144.80(6)
O(355)-La(2)-O(2)	69.19(5)
O(4)-La(2)-O(2)	69.07(5)
O(356)-La(2)-O(2)	119.47(6)
O(10)-La(2)-O(2)	67.60(6)
O(355)-La(2)-O(354)	71.43(7)
O(4)-La(2)-O(354)	146.23(4)

O(356)-La(2)-O(354)	71.90(6)
O(10)-La(2)-O(354)	78.46(5)
O(2)-La(2)-O(354)	130.11(6)
O(355)-La(2)-O(6)	142.44(4)
O(4)-La(2)-O(6)	68.22(5)
O(356)-La(2)-O(6)	72.70(5)
O(10)-La(2)-O(6)	132.50(5)
O(2)-La(2)-O(6)	129.23(5)
O(354)-La(2)-O(6)	100.64(6)
O(355)-La(2)-O(8)	132.99(6)
O(4)-La(2)-O(8)	129.25(5)
O(356)-La(2)-O(8)	114.65(6)
O(10)-La(2)-O(8)	68.34(5)
O(2)-La(2)-O(8)	125.87(4)
O(354)-La(2)-O(8)	66.93(5)
O(6)-La(2)-O(8)	67.98(5)
O(355)-La(2)-O(353)	139.00(6)
O(4)-La(2)-O(353)	82.04(7)
O(356)-La(2)-O(353)	145.60(7)
O(10)-La(2)-O(353)	68.92(6)
O(2)-La(2)-O(353)	72.63(7)
O(354)-La(2)-O(353)	127.47(7)
O(6)-La(2)-O(353)	75.50(6)
O(8)-La(2)-O(353)	63.24(7)
N(10)-Cu(1)-O(2)	90.56(8)

N(10)-Cu(1)-O(1)	169.14(8)
O(2)-Cu(1)-O(1)	84.90(7)
N(10)-Cu(1)-N(9)	82.34(9)
O(2)-Cu(1)-N(9)	172.29(9)
O(1)-Cu(1)-N(9)	101.58(9)
N(10)-Cu(1)-O(200)	98.15(8)
O(2)-Cu(1)-O(200)	94.40(6)
O(1)-Cu(1)-O(200)	92.04(7)
N(9)-Cu(1)-O(200)	89.58(7)
N(2)-Cu(2)-O(4)	92.13(8)
N(2)-Cu(2)-O(3)	176.42(8)
O(4)-Cu(2)-O(3)	84.98(7)
N(2)-Cu(2)-N(1)	82.94(9)
O(4)-Cu(2)-N(1)	171.90(9)
O(3)-Cu(2)-N(1)	100.17(8)
O(6)-Cu(3)-N(4)	91.27(7)
O(6)-Cu(3)-O(5)	85.44(7)
N(4)-Cu(3)-O(5)	174.36(6)
O(6)-Cu(3)-N(3)	172.65(8)
N(4)-Cu(3)-N(3)	81.55(8)
O(5)-Cu(3)-N(3)	101.84(8)
N(6)-Cu(4)-O(8)	91.52(8)
N(6)-Cu(4)-O(7)	175.02(6)
O(8)-Cu(4)-O(7)	85.15(7)
N(6)-Cu(4)-N(5)	82.39(8)

O(8)-Cu(4)-N(5)	173.28(8)
O(7)-Cu(4)-N(5)	100.75(8)
N(8)-Cu(5)-O(10)	91.92(8)
N(8)-Cu(5)-O(9)	174.57(8)
O(10)-Cu(5)-O(9)	84.79(8)
N(8)-Cu(5)-N(7)	83.31(9)
O(10)-Cu(5)-N(7)	169.90(6)
O(9)-Cu(5)-N(7)	100.60(9)
N(20)-Cu(6)-O(12)	91.53(8)
N(20)-Cu(6)-O(11)	175.58(9)
O(12)-Cu(6)-O(11)	84.87(8)
N(20)-Cu(6)-N(19)	81.71(10)
O(12)-Cu(6)-N(19)	173.10(10)
O(11)-Cu(6)-N(19)	101.94(10)
N(18)-Cu(7)-O(20)	90.99(7)
N(18)-Cu(7)-O(19)	174.19(8)
O(20)-Cu(7)-O(19)	84.64(7)
N(18)-Cu(7)-N(17)	83.15(8)
O(20)-Cu(7)-N(17)	173.88(9)
O(19)-Cu(7)-N(17)	101.10(8)
N(18)-Cu(7)-O(302)	89.62(7)
O(20)-Cu(7)-O(302)	97.28(7)
O(19)-Cu(7)-O(302)	94.72(7)
N(17)-Cu(7)-O(302)	84.48(8)
N(16)-Cu(8)-O(18)	91.18(8)

N(16)-Cu(8)-O(17)	175.94(8)
O(18)-Cu(8)-O(17)	85.10(7)
N(16)-Cu(8)-N(15)	82.66(8)
O(18)-Cu(8)-N(15)	172.56(6)
O(17)-Cu(8)-N(15)	101.17(8)
N(14)-Cu(9)-O(16)	90.58(8)
N(14)-Cu(9)-O(15)	168.06(6)
O(16)-Cu(9)-O(15)	85.29(7)
N(14)-Cu(9)-N(13)	81.96(9)
O(16)-Cu(9)-N(13)	172.35(9)
O(15)-Cu(9)-N(13)	101.68(8)
N(14)-Cu(9)-O(250)	98.49(7)
O(16)-Cu(9)-O(250)	91.77(6)
O(15)-Cu(9)-O(250)	92.84(6)
N(13)-Cu(9)-O(250)	91.04(6)
O(14)-Cu(10)-N(12)	91.40(9)
O(14)-Cu(10)-O(13)	85.66(8)
N(12)-Cu(10)-O(13)	175.22(7)
O(14)-Cu(10)-N(11)	167.94(9)
N(12)-Cu(10)-N(11)	82.66(10)
O(13)-Cu(10)-N(11)	100.91(9)
C(301)-S(1)-C(304)	91.17(15)
C(305)-S(2)-C(308)	91.95(16)
C(1)-O(1)-Cu(1)	107.11(17)
N(2)-O(2)-Cu(1)	109.02(12)

N(2)-O(2)-La(2)	122.40(10)
Cu(1)-O(2)-La(2)	125.48(9)
C(10)-O(3)-Cu(2)	108.19(14)
N(4)-O(4)-Cu(2)	109.43(13)
N(4)-O(4)-La(2)	123.39(13)
Cu(2)-O(4)-La(2)	126.80(7)
C(19)-O(5)-Cu(3)	107.77(14)
N(6)-O(6)-Cu(3)	109.16(11)
N(6)-O(6)-La(2)	123.06(12)
Cu(3)-O(6)-La(2)	125.71(8)
C(28)-O(7)-Cu(4)	107.51(16)
N(8)-O(8)-Cu(4)	108.54(14)
N(8)-O(8)-La(2)	120.84(13)
Cu(4)-O(8)-La(2)	123.06(6)
C(37)-O(9)-Cu(5)	108.37(14)
N(10)-O(10)-Cu(5)	109.97(13)
N(10)-O(10)-La(2)	123.75(13)
Cu(5)-O(10)-La(2)	125.12(8)
C(46)-O(11)-Cu(6)	107.46(18)
N(12)-O(12)-Cu(6)	109.74(16)
N(12)-O(12)-La(1)	120.77(13)
Cu(6)-O(12)-La(1)	122.63(8)
C(55)-O(13)-Cu(10)	107.67(14)
N(14)-O(14)-Cu(10)	109.07(12)
N(14)-O(14)-La(1)	124.08(13)

Cu(10)-O(14)-La(1)	124.71(9)
C(64)-O(15)-Cu(9)	107.42(15)
N(16)-O(16)-Cu(9)	108.51(13)
N(16)-O(16)-La(1)	123.24(12)
Cu(9)-O(16)-La(1)	125.09(7)
C(73)-O(17)-Cu(8)	108.11(14)
N(18)-O(18)-Cu(8)	109.10(12)
N(18)-O(18)-La(1)	122.47(13)
Cu(8)-O(18)-La(1)	126.63(6)
C(82)-O(19)-Cu(7)	107.73(15)
N(20)-O(20)-Cu(7)	108.84(12)
N(20)-O(20)-La(1)	121.12(10)
Cu(7)-O(20)-La(1)	124.51(8)
C(2)-N(1)-Cu(2)	111.72(18)
C(1)-N(2)-O(2)	114.16(18)
C(1)-N(2)-Cu(2)	119.09(18)
O(2)-N(2)-Cu(2)	126.64(13)
C(11)-N(3)-Cu(3)	111.24(12)
C(10)-N(4)-O(4)	114.21(19)
C(10)-N(4)-Cu(3)	119.30(15)
O(4)-N(4)-Cu(3)	125.41(15)
C(20)-N(5)-Cu(4)	112.32(16)
C(19)-N(6)-O(6)	114.61(19)
C(19)-N(6)-Cu(4)	119.75(18)
O(6)-N(6)-Cu(4)	125.63(13)

C(29)-N(7)-Cu(5)	110.57(16)
C(28)-N(8)-O(8)	114.51(18)
C(28)-N(8)-Cu(5)	119.39(15)
O(8)-N(8)-Cu(5)	126.10(16)
C(38)-N(9)-Cu(1)	112.96(16)
C(37)-N(10)-O(10)	114.6(2)
C(37)-N(10)-Cu(1)	119.48(17)
O(10)-N(10)-Cu(1)	125.83(15)
C(47)-N(11)-Cu(10)	111.97(16)
C(46)-N(12)-O(12)	114.9(2)
C(46)-N(12)-Cu(10)	118.88(17)
O(12)-N(12)-Cu(10)	126.20(18)
C(56)-N(13)-Cu(9)	112.00(15)
C(55)-N(14)-O(14)	114.1(2)
C(55)-N(14)-Cu(9)	120.20(18)
O(14)-N(14)-Cu(9)	125.70(14)
C(65)-N(15)-Cu(8)	110.59(16)
C(64)-N(16)-O(16)	115.20(17)
C(64)-N(16)-Cu(8)	118.85(15)
O(16)-N(16)-Cu(8)	125.63(14)
C(74)-N(17)-Cu(7)	111.91(14)
C(73)-N(18)-O(18)	115.32(19)
C(73)-N(18)-Cu(7)	118.04(15)
O(18)-N(18)-Cu(7)	126.60(14)
C(83)-N(19)-Cu(6)	111.48(18)

C(82)-N(20)-O(20)	114.5(2)
C(82)-N(20)-Cu(6)	120.37(19)
O(20)-N(20)-Cu(6)	125.03(14)
O(1)-C(1)-N(2)	124.1(3)
O(1)-C(1)-C(2)	120.3(2)
N(2)-C(1)-C(2)	115.6(2)
N(1)-C(2)-C(1)	109.4(2)
N(1)-C(2)-C(3)	111.96(18)
C(1)-C(2)-C(3)	111.3(2)
C(0A)-C(3)-C(4)	9.88(17)
C(0A)-C(3)-C(2)	112.1(3)
C(4)-C(3)-C(2)	111.6(2)
C(9)-C(4)-C(5)	115.9(3)
C(9)-C(4)-C(3)	121.0(3)
C(5)-C(4)-C(3)	123.0(2)
C(6)-C(5)-C(4)	120.3(3)
C(5)-C(6)-C(7)	121.8(4)
C(8)-C(7)-C(6)	117.9(4)
C(7)-C(8)-C(9)	119.5(3)
C(4)-C(9)-C(8)	124.5(3)
C(0F)-C(0A)-C(0B)	126.5(6)
C(0F)-C(0A)-C(3)	118.6(4)
C(0B)-C(0A)-C(3)	114.9(4)
C(0A)-C(0B)-C(0C)	113.4(5)
C(0D)-C(0C)-C(0B)	121.7(6)

C(0E)-C(0D)-C(0C)	121.8(8)
C(0D)-C(0E)-C(0F)	117.9(6)
C(0A)-C(0F)-C(0E)	118.3(5)
O(3)-C(10)-N(4)	123.10(19)
O(3)-C(10)-C(11)	121.6(2)
N(4)-C(10)-C(11)	115.1(2)
N(3)-C(11)-C(10)	108.3(2)
N(3)-C(11)-C(12)	113.53(15)
C(10)-C(11)-C(12)	111.1(2)
C(13)-C(12)-C(11)	110.8(2)
C(18)-C(13)-C(14)	117.5(3)
C(18)-C(13)-C(12)	122.6(3)
C(14)-C(13)-C(12)	119.9(2)
C(15)-C(14)-C(13)	122.3(2)
C(14)-C(15)-C(16)	118.1(3)
C(17)-C(16)-C(15)	120.4(3)
C(16)-C(17)-C(18)	121.4(3)
C(13)-C(18)-C(17)	120.3(3)
O(5)-C(19)-N(6)	122.9(2)
O(5)-C(19)-C(20)	121.70(19)
N(6)-C(19)-C(20)	115.3(2)
N(5)-C(20)-C(19)	109.32(18)
N(5)-C(20)-C(21)	112.69(19)
C(19)-C(20)-C(21)	111.39(18)
C(22)-C(21)-C(20)	113.02(18)

C(27)-C(22)-C(23)	117.8(3)
C(27)-C(22)-C(21)	120.7(3)
C(23)-C(22)-C(21)	121.5(3)
C(22)-C(23)-C(24)	121.3(3)
C(23)-C(24)-C(25)	119.6(3)
C(26)-C(25)-C(24)	119.4(4)
C(25)-C(26)-C(27)	120.1(3)
C(22)-C(27)-C(26)	121.8(3)
O(7)-C(28)-N(8)	123.7(2)
O(7)-C(28)-C(29)	122.0(2)
N(8)-C(28)-C(29)	114.2(2)
N(7)-C(29)-C(28)	110.2(2)
N(7)-C(29)-C(30)	113.1(2)
C(28)-C(29)-C(30)	110.33(18)
C(31)-C(30)-C(29)	111.63(19)
C(32)-C(31)-C(36)	117.3(4)
C(32)-C(31)-C(30)	123.3(3)
C(36)-C(31)-C(30)	119.2(3)
C(31)-C(32)-C(33)	122.9(4)
C(34)-C(33)-C(32)	119.3(4)
C(35)-C(34)-C(33)	121.2(5)
C(34)-C(35)-C(36)	120.4(6)
C(31)-C(36)-C(35)	117.4(5)
O(9)-C(37)-N(10)	122.1(2)
O(9)-C(37)-C(38)	122.2(2)

N(10)-C(37)-C(38)	115.7(2)
N(9)-C(38)-C(37)	109.14(19)
N(9)-C(38)-C(39)	112.6(3)
C(37)-C(38)-C(39)	111.8(2)
C(40)-C(39)-C(38)	112.6(3)
C(45)-C(40)-C(41)	118.3(3)
C(45)-C(40)-C(39)	121.5(2)
C(41)-C(40)-C(39)	120.1(3)
C(40)-C(41)-C(42)	120.5(3)
C(41)-C(42)-C(43)	120.9(3)
C(44)-C(43)-C(42)	118.8(3)
C(43)-C(44)-C(45)	119.7(4)
C(40)-C(45)-C(44)	121.7(3)
O(11)-C(46)-N(12)	122.9(2)
O(11)-C(46)-C(47)	121.1(3)
N(12)-C(46)-C(47)	115.9(2)
N(11)-C(47)-C(48)	112.80(19)
N(11)-C(47)-C(46)	108.4(2)
C(48)-C(47)-C(46)	113.7(3)
C(5A)-C(48)-C(47)	113.8(3)
C(5A)-C(48)-C(49)	18.1(3)
C(47)-C(48)-C(49)	110.6(3)
C(54)-C(49)-C(50)	121.0(5)
C(54)-C(49)-C(48)	120.8(3)
C(50)-C(49)-C(48)	118.2(4)

C(51)-C(50)-C(49)	115.9(5)
C(52)-C(51)-C(50)	122.8(5)
C(51)-C(52)-C(53)	120.7(6)
C(54)-C(53)-C(52)	118.1(7)
C(53)-C(54)-C(49)	121.3(5)
C(5F)-C(5A)-C(5B)	126.1(5)
C(5F)-C(5A)-C(48)	115.9(5)
C(5B)-C(5A)-C(48)	117.8(4)
C(5A)-C(5B)-C(5C)	114.3(6)
C(5D)-C(5C)-C(5B)	118.4(7)
C(5C)-C(5D)-C(5E)	124.6(7)
C(5D)-C(5E)-C(5F)	117.8(6)
C(5E)-C(5F)-C(5A)	116.8(6)
N(14)-C(55)-O(13)	123.5(2)
N(14)-C(55)-C(56)	114.3(2)
O(13)-C(55)-C(56)	122.1(2)
N(13)-C(56)-C(55)	108.53(19)
N(13)-C(56)-C(57)	112.62(19)
C(55)-C(56)-C(57)	111.3(2)
C(58)-C(57)-C(56)	109.8(2)
C(63)-C(58)-C(59)	120.0(4)
C(63)-C(58)-C(57)	121.0(3)
C(59)-C(58)-C(57)	119.0(3)
C(60)-C(59)-C(58)	119.4(4)
C(61)-C(60)-C(59)	119.1(4)

C(60)-C(61)-C(62)	123.5(4)
C(63)-C(62)-C(61)	116.6(4)
C(58)-C(63)-C(62)	121.4(3)
O(15)-C(64)-N(16)	123.2(2)
O(15)-C(64)-C(65)	121.5(2)
N(16)-C(64)-C(65)	115.29(18)
N(15)-C(65)-C(64)	109.1(2)
N(15)-C(65)-C(66)	112.4(2)
C(64)-C(65)-C(66)	110.51(16)
C(67)-C(66)-C(65)	113.64(16)
C(68)-C(67)-C(72)	117.4(3)
C(68)-C(67)-C(66)	122.0(3)
C(72)-C(67)-C(66)	120.6(3)
C(67)-C(68)-C(69)	120.1(3)
C(70)-C(69)-C(68)	120.8(3)
C(69)-C(70)-C(71)	118.8(3)
C(72)-C(71)-C(70)	121.1(4)
C(71)-C(72)-C(67)	121.7(3)
N(18)-C(73)-O(17)	122.31(19)
N(18)-C(73)-C(74)	117.4(2)
O(17)-C(73)-C(74)	120.3(2)
N(17)-C(74)-C(73)	109.4(2)
N(17)-C(74)-C(7G)	115.6(3)
C(73)-C(74)-C(7G)	110.0(2)
N(17)-C(74)-C(75)	107.2(3)

C(73)-C(74)-C(75)	109.3(2)
C(7G)-C(74)-C(75)	10.2(3)
O(19)-C(82)-N(20)	123.8(3)
O(19)-C(82)-C(83)	122.0(2)
N(20)-C(82)-C(83)	114.2(2)
N(19)-C(83)-C(82)	109.5(2)
N(19)-C(83)-C(84)	112.9(2)
C(82)-C(83)-C(84)	111.0(2)
C(85)-C(84)-C(83)	111.2(3)
C(86)-C(85)-C(90)	119.6(4)
C(86)-C(85)-C(84)	121.5(3)
C(90)-C(85)-C(84)	118.9(3)
C(85)-C(86)-C(87)	119.7(4)
C(88)-C(87)-C(86)	121.2(4)
C(87)-C(88)-C(89)	121.6(4)
C(88)-C(89)-C(90)	119.1(3)
C(89)-C(90)-C(85)	118.8(3)
C(200)-O(200)-C(20A)	45.5(4)
C(200)-O(200)-Cu(1)	135.6(2)
C(20A)-O(200)-Cu(1)	119.0(2)
O(200)-C(200)-O(201)	120.6(4)
O(200)-C(200)-C(201)	121.2(4)
O(201)-C(200)-C(201)	118.0(5)
C(202)-C(201)-C(200)	127.2(5)
C(202)-C(201)-S(3)	114.8(4)

C(200)-C(201)-S(3)	118.0(4)
C(201)-C(202)-C(203)	112.7(6)
C(202)-C(203)-C(204)	110.6(6)
C(205)-C(204)-C(203)	126.6(5)
C(205)-C(204)-S(3)	123.7(4)
C(203)-C(204)-S(3)	109.1(3)
C(201)-S(3)-C(204)	92.3(3)
C(205)-S(4)-C(208)	89.5(2)
C(206)-C(205)-C(204)	128.8(4)
C(206)-C(205)-S(4)	110.4(3)
C(204)-C(205)-S(4)	120.6(4)
C(205)-C(206)-C(207)	112.9(5)
C(208)-C(207)-C(206)	116.0(6)
C(207)-C(208)-C(209)	137.1(6)
C(207)-C(208)-S(4)	109.9(4)
C(209)-C(208)-S(4)	112.9(4)
O(203)-C(209)-O(202)	122.2(5)
O(203)-C(209)-C(208)	121.7(4)
O(202)-C(209)-C(208)	115.4(5)
C(215)-N(215)-C(216)	122.9(7)
C(215)-N(215)-C(217)	122.5(5)
C(216)-N(215)-C(217)	114.5(7)
O(215)-C(215)-N(215)	120.8(4)
C(76)-C(75)-C(74)	113.9(4)
C(77)-C(76)-C(81)	121.3(5)

C(77)-C(76)-C(75)	120.6(5)
C(81)-C(76)-C(75)	118.0(4)
C(76)-C(77)-C(78)	114.1(6)
C(79)-C(78)-C(77)	121.4(6)
C(78)-C(79)-C(80)	124.0(6)
C(79)-C(80)-C(81)	114.3(6)
C(80)-C(81)-C(76)	123.2(5)
O(20A)-C(20A)-O(200)	129.4(4)
O(20A)-C(20A)-C(20B)	116.7(5)
O(200)-C(20A)-C(20B)	113.9(3)
C(20C)-C(20B)-C(20A)	129.1(4)
C(20C)-C(20B)-S(3A)	111.5(3)
C(20A)-C(20B)-S(3A)	119.3(4)
C(20B)-C(20C)-C(20D)	112.5(5)
C(20E)-C(20D)-C(20C)	112.7(6)
C(20D)-C(20E)-C(20F)	130.3(5)
C(20D)-C(20E)-S(3A)	111.4(3)
C(20F)-C(20E)-S(3A)	118.2(4)
C(20E)-S(3A)-C(20B)	91.8(2)
C(20F)-S(4A)-C(20I)	93.1(2)
C(20E)-C(20F)-C(20G)	129.8(5)
C(20E)-C(20F)-S(4A)	119.8(4)
C(20G)-C(20F)-S(4A)	109.7(3)
C(20H)-C(20G)-C(20F)	105.9(5)
C(20I)-C(20H)-C(20G)	123.5(5)

C(20H)-C(20I)-C(20J)	134.1(5)
C(20H)-C(20I)-S(4A)	107.0(3)
C(20J)-C(20I)-S(4A)	118.9(4)
O(20C)-C(20J)-O(20B)	123.7(5)
O(20C)-C(20J)-C(20I)	115.7(5)
O(20B)-C(20J)-C(20I)	119.9(4)
O(21A)-C(21A)-N(21A)	132.7(6)
C(21A)-N(21A)-C(21B)	124.8(5)
C(21A)-N(21A)-C(21C)	116.9(5)
C(21B)-N(21A)-C(21C)	118.2(5)
C(7A)-C(7G)-C(74)	115.0(3)
C(7B)-C(7A)-C(7F)	119.0(3)
C(7B)-C(7A)-C(7G)	118.6(4)
C(7F)-C(7A)-C(7G)	122.5(4)
C(7A)-C(7B)-C(7C)	119.8(4)
C(7D)-C(7C)-C(7B)	120.0(5)
C(7E)-C(7D)-C(7C)	118.4(4)
C(7F)-C(7E)-C(7D)	122.6(5)
C(7E)-C(7F)-C(7A)	120.2(4)
C(250)-O(250)-Cu(9)	128.97(15)
O(251)-C(250)-O(250)	126.5(2)
O(251)-C(250)-C(251)	117.33(16)
O(250)-C(250)-C(251)	116.1(2)
C(252)-C(251)-C(250)	130.9(2)
C(252)-C(251)-S(5)	109.6(2)

C(250)-C(251)-S(5)	119.41(13)
C(251)-C(252)-C(253)	114.7(3)
C(254)-C(253)-C(252)	113.0(2)
C(253)-C(254)-C(255)	130.8(2)
C(253)-C(254)-S(5)	110.8(2)
C(255)-C(254)-S(5)	118.37(15)
C(251)-S(5)-C(254)	91.97(10)
C(258)-S(6)-C(255)	92.67(11)
C(256)-C(255)-C(254)	128.96(18)
C(256)-C(255)-S(6)	110.46(18)
C(254)-C(255)-S(6)	120.58(15)
C(255)-C(256)-C(257)	112.7(2)
C(258)-C(257)-C(256)	114.2(2)
C(257)-C(258)-C(259)	129.4(2)
C(257)-C(258)-S(6)	110.0(2)
C(259)-C(258)-S(6)	120.57(16)
O(252)-C(259)-O(253)	124.2(2)
O(252)-C(259)-C(258)	119.3(2)
O(253)-C(259)-C(258)	116.5(2)
C(309)-O(302)-Cu(7)	112.56(15)
O(301)-C(300)-O(300)	126.5(2)
O(301)-C(300)-C(301)	118.1(3)
O(300)-C(300)-C(301)	115.3(3)
C(302)-C(301)-C(300)	130.9(3)
C(302)-C(301)-S(1)	112.1(2)

C(300)-C(301)-S(1)	117.0(2)
C(301)-C(302)-C(303)	111.9(3)
C(304)-C(303)-C(302)	113.9(3)
C(303)-C(304)-C(305)	130.9(3)
C(303)-C(304)-S(1)	111.0(2)
C(305)-C(304)-S(1)	118.1(3)
C(306)-C(305)-C(304)	125.1(3)
C(306)-C(305)-S(2)	111.4(3)
C(304)-C(305)-S(2)	123.5(2)
C(305)-C(306)-C(307)	110.2(4)
C(308)-C(307)-C(306)	113.9(3)
C(307)-C(308)-C(309)	130.7(3)
C(307)-C(308)-S(2)	112.4(3)
C(309)-C(308)-S(2)	116.9(2)
O(303)-C(309)-O(302)	127.1(3)
O(303)-C(309)-C(308)	118.9(3)
O(302)-C(309)-C(308)	114.0(3)
La(1)-O(353)-La(2)	169.61(12)
O(420)-C(420)-N(420)	125.9(10)
C(420)-N(420)-C(421)	125.3(8)
C(420)-N(420)-C(422)	118.9(8)
C(421)-N(420)-C(422)	115.7(6)
O(423)-C(423)-N(423)	126.2(7)
C(423)-N(423)-C(424)	127.6(7)
C(423)-N(423)-C(425)	116.5(7)

C(424)-N(423)-C(425)	115.7(6)
O(427)-C(427)-N(427)	126.9(7)
C(427)-N(427)-C(428)	119.3(6)
C(427)-N(427)-C(429)	121.6(7)
C(428)-N(427)-C(429)	119.1(6)
O(500)-C(500)-N(500)	120.9(4)
C(500)-N(500)-C(501)	122.6(4)
C(500)-N(500)-C(502)	120.1(4)
C(501)-N(500)-C(502)	117.3(4)
C(50B)-C(50A)-O(50A)	105.0(8)
C(505)-N(505)-C(507)	124.0(6)
C(505)-N(505)-C(506)	118.3(4)
C(507)-N(505)-C(506)	117.3(5)
O(505)-C(505)-N(505)	115.0(4)
C(515)-N(515)-C(516)	123.4(3)
C(515)-N(515)-C(517)	119.0(3)
C(516)-N(515)-C(517)	117.5(3)
O(515)-C(515)-N(515)	121.5(3)
C(525)-N(525)-C(526)	122.6(7)
C(525)-N(525)-C(527)	120.8(6)
C(526)-N(525)-C(527)	116.5(4)
O(525)-C(525)-N(525)	124.0(11)
C(530)-N(530)-C(531)	126.2(5)
C(530)-N(530)-C(532)	113.7(7)
C(531)-N(530)-C(532)	115.6(5)

O(530)-C(530)-N(530)	131.7(5)
C(540)-N(540)-C(541)	120.9(3)
C(540)-N(540)-C(542)	123.5(3)
C(541)-N(540)-C(542)	115.6(3)
O(540)-C(540)-N(540)	126.3(3)
C(550)-N(550)-C(551)	117.6(4)
C(550)-N(550)-C(552)	119.2(3)
C(551)-N(550)-C(552)	122.9(4)
O(550)-C(550)-N(550)	122.9(4)
C(560)-N(560)-C(562)	119.0(4)
C(560)-N(560)-C(561)	119.1(4)
C(562)-N(560)-C(561)	121.9(4)
O(560)-C(560)-N(560)	123.5(4)
O(570)-C(570)-N(570)	123.9(5)
C(570)-N(570)-C(571)	124.5(4)
C(570)-N(570)-C(572)	121.1(3)
C(571)-N(570)-C(572)	114.2(4)
C(590)-N(590)-C(592)	122.4(3)
C(590)-N(590)-C(591)	119.8(3)
C(592)-N(590)-C(591)	117.8(2)
O(590)-C(590)-N(590)	124.1(3)
O(70A)-C(70A)-N(70A)	138.6(11)
C(70A)-N(70A)-C(70B)	120.4(7)
C(70A)-N(70A)-C(70C)	112.4(6)
C(70B)-N(70A)-C(70C)	111.8(5)